



**POLYTECHNIC UNIVERSITY
POLITEHNICA OF BUCHAREST**

**Faculty of Mechanical Engineering and
Mechatronics**

Department of Thermotechnics, Engines, Thermal and
Refrigeration Equipment



PhD THESIS

**RESEARCHES REGARDING THE USE OF LPG TO THE CAR DIESEL
ENGINE**

Author: engineer Liviu-Alberto NEMOIANU

Scientific coordinator: professor emeritus doctor engineer Constantin PANĂ

BUCHAREST
2022

University Politehnica of Bucharest
Faculty of Mechanical Engineering and Mechatronics, Department of Thermotechnics,
Engines, Thermal and Refrigeration Equipment

Thesis title: **Researches regarding the use of LPG to the car diesel engine**

Author: eng. Liviu Alberto Nemoianu

Doctorate scientific coordinator: prof. univ. emeritus PhD. eng. Constantin Pană

KEY WORDS: diesel engine; combustion; pollutant emissions; modelling; liquefied petroleum gas (LPG); nitrous oxides; smoke.

ABSTRACT OF THE THESIS:

CONTENT

CHAPTER I	3
1. RELEVANCE OF THE RESEARCH TOPIC. THE OBJECTIVES OF THE WORK	3
1.1. INTRODUCTION	3
1.2. RELEVANCE OF THE RESEARCH THEME	3
1.3. LPG PROPERTIES. IMPLICATIONS ON LPG DIESEL ENGINE OPERATION	3
1.4. LPG FUELING METHODS FOR DIESEL ENGINE.....	4
1.5. MANUFACTURING PROCESSES OF LPG	4
1.6. OBJECTIVES OF THE DOCTORAL THESIS	4
CHAPTER II	4
2. ANALYSIS OF THE CURRENT STATE OF RESEARCH IN THE FIELD	4
2.1. CURRENT STATE OF RESEARCH IN THE FIELD	4
2.2. CONCLUSIONS	5
CHAPTER III	5
3. EXPERIMENTAL INVESTIGATIONS OF LPG FUEL DIESEL ENGINE	5
3.1. LABORATORY EQUIPMENT AND EQUIPMENT. WORKING PROCEDURE	5
3.1.1. K9K compression ignition engine	5
3.1.2. Eddy-current electric dyno	5
3.1.3. Actuator of the load adjuster.....	6
3.1.4. Dyno coupling shaft	6
3.1.5. Thermoresistances and thermocouples for temperatures measurement.....	6
3.1.6. The pressure gauge for the supercharging pressure measurement.....	6
3.1.7. Determination of the air consumption	6
3.1.8. Determination of the fuel consumption	6
3.1.9. Data acquisition system	6
3.1.10. Equipment for measuring the level of pollutant emissions and greenhouse gases in exhaust gases	6
3.1.11. Organization of the experimental test bed	7
3.1.12. Working procedure	7
3.1.13. Diagnosis and repair of electric dyno HORIBA SCHENCK E90	7
3.2. RESULTS OF EXPERIMENTAL INVESTIGATIONS	8
3.2.1. Establishing the degree of substitution of diesel fuel with liquefied petroleum gas	8
3.2.2. The study of the influence of the degree of substitution on the specific energy consumption	8
3.2.3. Study of the influence of the degree of substitution on the mechanical demands of the engine. Maximum pressure. Maximum pressure rise rate	10
3.2.4. The study of the influence of the degree of substitution on the level of pollutant emissions of the car diesel engine fuelled with liquefied petroleum gas	11
3.2.5. Study of the influence of the degree of substitution on the cyclic variability of the combustion process in the car diesel engine fuelled with liquefied petroleum gas	13
3.3. CONCLUSIONS OF EXPERIMENTAL INVESTIGATIONS	18

CHAPTER IV	19
4. MODELING OF THERMOGASODYNAMICAL PROCESSES IN THE CYLINDER OF THE LPG-FUELED DIESEL ENGINE	19
4.1. MODELING OF THERMOGASODYNAMICAL PROCESSES IN THE ENGINE CYLINDER - MUSA MODEL	19
4.1.1. Hypotheses	19
4.1.2. Gas exchange processes	19
4.1.3. Compression process	19
4.1.4. Combustion process	19
4.1.5. Expansion process	19
4.1.6. The results of the simulation of thermo-gas-dynamic processes	19
4.2. MODELING OF THE DIESEL FUEL VAPORATION, MIXTURE FORMATION AND COMBUSTION PROCESSES WITH A DEVELOPED ZERO DIMENSIONAL UNIZONE PHYSICAL-MATHEMATICAL MODEL – SVAP MODEL	21
CHAPTER V	26
5. COMPARATIVE ANALYSIS OF THE RESULTS OF EXPERIMENTAL AND THEORETICAL INVESTIGATIONS	26
5.1. COMPARISON BETWEEN THEORETICAL (MODELING OF THERMOGASODYNAMICAL PROCESSES IN THE K9K DIESEL ENGINE CYLINDER) AND EXPERIMENTAL RESULTS	26
5.1.1. In-cylinder pressure	26
5.1.2. The combustion law	27
5.1.3. The NO_x emission level	27
5.1.4. The smoke emission level	28
5.2. COMPARISON BETWEEN THE RESULTS OBTAINED THROUGH THE MODELING OF THERMOGASODYNAMICAL PROCESSES IN THE K9K ENGINE CYLINDER WITH THE AVL BOOST MODEL AND THE EXPERIMENTAL RESULTS	28
5.3. CONCLUSIONS	29
CHAPTER VI	29
6. CONCLUSIONS, PERSONAL CONTRIBUTIONS, FUTURE RESEARCH DIRECTIONS. DISSEMINATION OF THE CARRIED OUT RESEARCH RESULTS	29
6.1. CONCLUSIONS	29
6.2. PERSONAL CONTRIBUTIONS	30
6.3. FUTURE RESEARCH DIRECTIONS	30
SELECTIVE BIBLIOGRAPHY	30

CHAPTER I

1. RELEVANCE OF THE RESEARCH TOPIC. OBJECTIVES OF THE WORK

1.1. INTRODUCTION

In general, the reduction in the level of polluting emissions from internal combustion engines exhaust gases, in particular from compression ignition engines, is required by increasingly stringent regulations issued by the European Commission in the global context of environmental protection. The exhaust gases of diesel engines contain pollutants with various harmful actions, the regulated ones being: unburned hydrocarbons (HC), carbon monoxide, (CO), nitrogen oxides, (NO_x), particles, smoke and carbon dioxide (CO₂), which is considered as a greenhouse gas.

1.2. RELEVANCE OF THE RESEARCH TOPIC

The sharp reduction in petrol reserves around the world calls for the use of alternative fuels, especially from sustainable and renewable resources [6].

1.3. LPG PROPERTIES. IMPLICATIONS FOR THE OPERATION OF THE LPG-FUELLED DIESEL ENGINE

The standard fuel used in compression ignition engines for motor vehicles is the diesel fuels, (diesel fuel is a hydrocarbon mixtures with 12... 20 carbon atoms in the molecule obtained by primary distillation of petroleum).

Liquefied petroleum gas is a mixture of butane (C₄H₁₀) and propane (C₃H₈). In general, the proportion is 50% propane and 50% butane; the composition may differ depending on the season (when

the temperature is lower the proportion of propane increases due to its lower boiling temperature) and the geographical area.

1.4. LPG DIESEL ENGINE FUELLING METHODS

The following LPG fuelling methods are known [9], [12], [14]: MAS-LPG; diesel-gas; LPG direct injection; double injection.

The diesel-gas process. The LPG is injected into the intake manifold and the air-LPG mixture ignites from the flame initiated by a diesel pilot. The diesel engine is equipped with two fuelling systems: a standard one, which provides the injection of the diesel pilot and an LPG fuelling system equipped with a evaporator and pressure regulator.

In conclusion, the LPG fuelling of diesel engines offers the following advantages,[9] [9] [21]: reducing the level of pollutant emissions; reducing of the specific energy consumption; reducing of the engine noise; significantly increasing of the engine reliability; reducing of the costs for engine maintenance; protection of the particulate filter.

Of all the LPG fuelling methods, the author chose the diesel-gas process due to its advantages.

1.5. LPG MANUFACTURING PROCESSES

Liquefied petroleum gas is a mixture of gaseous hydrocarbons, propane and butane being the main components. Propylene and butylene are also found in the gaseous mixture in small proportions. The international standard for LPG is EN 589, also adopted in Romania as SR EN 589, [23].

The LPG - liquefied petroleum gas is obtained from the processing of crude petrol, natural gas, well gas, coal processing, [24].

1.6. OBJECTIVES OF THE THESIS

The main objective of the thesis is the use of LPG in the diesel engine of the car in order to increase the energy and pollution performance.

The specific objectives of the elaborated work were: *Analysis of the knowledge stage in the field; Adapting the K9K-792 diesel engine to the dual operation with two fuels, diesel and LPG; Diagnosis and upgrade of the Horiba Schenck E90 electric dyno; Modernization of the experimental test bed of the diesel engine and carrying out experimental investigations; Increasing the energy performance of the diesel engine by LPG fuelling in dual system; Reducing the level of polluting emissions from the exhaust gases of the engine by LPG fuelling in dual system; Modelling of thermos-gas-dynamic processes in the cylinder of the diesel engine fuelled with LPG in dual mode; Analysis of the results of theoretical and experimental research carried out on the diesel engine fuelled by LPG. Validation of the physical-mathematical model.*

CHAPTER II

2. ANALYSIS OF THE CURRENT STATE OF RESEARCH IN THE FIELD

The use of alternative fuels, either as single fuels or as partial substitutes for classical fuels, is a viable solution to reduce the level of pollutant emissions and greenhouse gases of the diesel engine. This can ensure that vehicles equipped with diesel engines are maintained in urban operation, a solution that responds to some of the problems discussed at the C40 Mayors' Summit held in Paris in 2016.

2.1. CURRENT STATE OF RESEARCH IN THE FIELD

To date, numerous researchers have conducted theoretical and experimental studies on the use of LPG to fuel the compression ignition engine. According to the *Institut Français du Pétrole (IFP)* for ten European cars equipped with diesel and LPG engines, the level of CO, HC, NO_x, PM emissions is reduced by 30% compared to diesel operation under similar test conditions [28].

Selim studied flammability limits and the possibility of "diesel detonation" when using LPG in a dual-cylinder Ricardo diesel engine and LPG-fuelled Ricardo engine. Noticing the increase in the actual engine torque with the increase in the amount of LPG, the LPG flow rate was gradually increased until the engine began to operate brutally, throbbing, *figure 2.1*, especially at low values of the engine torque, the influences being given by the low value of the low auto-ignition temperature of the LPG [47], [48]. High cyclic doses of LPG may increase the duration of the diesel pilot's self-ignition delay, which may lead to an increase in the pressure rise rate during combustion, *figure 2.1.(b)*, [37], [38], [39], [49], [50].

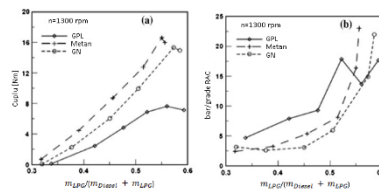


Fig. 2.1. Effects of the increase in the mass quantity of LPG on the engine torque (a) and the rate of increase in pressure (b); $n = 1300$ rpm, compression ratio 20, injection advance = 35 °RAC, $Ch_{diesel} = 0,37$ kg/h [49].

The duration of the diesel pilot's auto-ignition delay is influenced, among other things, by the presence of liquefied petroleum gas [51], *figure 2.2.*

When studying the operation of a diesel 4-cylinder engine fuelled by diesel fuel and LPG, *Stewart* discovered that for diesel fuel, the heat release speed has a specific allure characterized by a lower first maximum, followed by a second, more important maxim that occurs later on the cycle, but when using propane (component of LPG) and diesel fuel, the allure of the heat release rate changes, *figure 2.3.*, the phase of diffuse combustion having a more important share.

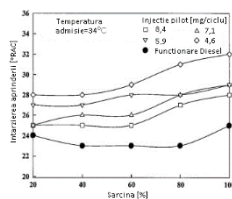


Fig. 2.2. Effect of the load on self-ignition delay [52].

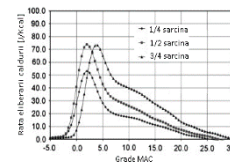


Fig. 2.3. The rate of heat release depending on the angle of rotation of the crankshaft when using propane-diesel fuels, at different loads and the speed of 1500 rpm [53].

2.2. CONCLUSIONS

The study based on the results obtained by different researchers in the field regarding the use of liquefied petroleum gas as an alternative fuel to the diesel engine allows for general conclusions to be drawn. Thus, when the diesel engine is supplied in a dual system, with diesel fuel and LPG, compared to the standard diesel fuelling, the following influences appear: *the reduction of the effective efficiency and the increase of the level of HC emissions at partial loads, aspects that can be improved by changing the condition conditions for the fresh load; the increase of the actual efficiency at high loads; the reduction of the NO_x emission level at partial loads and the significant reduction of the emission level of the emission of PM particles at all load regimes; increase in the maximum rate of increase in pressure during combustion as the cyclic dose of LPG increases and the dose for diesel fuelling remains constant; the increase in the total duration of the combustion process, especially at low loads, due to the increase in the duration of the delay in self-ignition; increasing the actual efficiency at high speed regimes; reduction of the maximum speed of increase in pressure during combustion when increasing engine speed; the use of a large cyclical diesel fuel dose ensures a reduction in the level of HC and CO emissions, but leads to an increase in the level of NO_x emission due to the increase in the overall temperature in the combustion chamber.*

CHAPTER III

3. EXPERIMENTAL INVESTIGATIONS OF THE LPG-FUELLED DIESEL ENGINE

The activities necessary to achieve the objectives of the work were: *adaptation of the diesel engine for diesel fuel and LPG fuelling; modernization of the experimental test bed; development of a methodology for conducting experimental investigations at the test stand of diesel engine powered by diesel and LPG; conducting experimental investigations; acquisition, processing and interpretation of experimental data.*

3.1. LABORATORY EQUIPMENT AND MACHINERY. WORKING PROCEDURE

3.1.1 Compression ignition engine K9K

The diesel-gas method is used for the dual fuelling with diesel fuel and LPG to the compression ignition engine type K9K 792 1.5 dCi that equips the Dacia car.

For operation in dual mode, with diesel fuel and LPG, the diesel engine is equipped with a second LPG injection fuelling system, a fuelling system that is electronically connected with the classic diesel fuelling system, thus designing a dual fuelling system.

3.1.2. Eddy-current electric dyno

To determine the operating regime of the engine, the test bed is equipped with an eddy-current electric dyno *Horiba Schenck E90.*

For the control of the electric dyno, a power unit and a control unit are used, from which the operating mode of the dyno (constant speed, constant torque) and the adjustment of the operating mode of the engine can be chosen. The control unit allows real-time visualization of the functional parameters of the engine such as speed, effective torque, effective power, but also of some auxiliary parameters: the position of the load actuator [96].

3.1.3. Actuator of the load adjuster

For the adjustment and control of the operating regime of the diesel engine, an electric actuator is used to regulate the position of the load adjusting organ. The electric actuator, model *Horiba – LMF2003* is controlled from the dyno control unit, being driven by a power unit, model *Horiba LFE2003* [3], connected to the dyno electric circuit. By means of a cable the actuator establishes the position of the accelerator pedal in accordance with the chosen operating mode, [96].

3.1.4. Dyno coupling shaft

The *E90* electric dyno connected with the diesel engine via an elastic coupling shaft model *Voith 190*. For reasons of safety operation, the coupling shaft is enclosed in a protective metal housing. When assembling the coupling between the diesel engine and the dyno, the difficulty of the assembly operation is given by the necessity of strictly fulfilling the deviations imposed by the manufacturer so that the operation of the engine-coupling-dyno assembly is carried out safely.

3.1.5. Thermoresistances and thermocouples for temperatures measurement

In order to monitor the thermal regime of the engine during the experimental tests, in order to maintain it in the range of normal values of the thermal regime that ensures safe operation and to achieve the performances specified by the construction plant, thermoresistors and thermocouples were installed in the intake system, exhaust system, oil and cooling systems. Heat resistors and thermocouples are coupled via electrical connections to *Shimaden SR93* digital type indicators, [97].

3.1.6. The pressure gauge for the supercharging pressure measurement

The supercharger pressure is determined by measuring with an *FSE 101-5* elastic bellows type manometer that is coupled by means of a pipe with the engine intake system.

3.1.7. Determination of the air consumption

An air flow meter mounted in the inlet section of the engine intake system before the air tank shall be used to determine the air consumption. The air tank has the role of cushioning the pressure oscillations in the intake system so that they do not adversely influence the determination of the engine's air consumption. The minimum required volume of the air tank (0,5 m³) is determined on the basis of a calculation relationship which takes into account the total cylinder capacity of the engine and the minimum idling speed, the volume of the air tank used being suitable for the K9K engine. The air flow meter used is of the *Krohne H250* rotameter type.

3.1.8. Determination of the fuel consumption

The determination of fuel consumption is carried out for each fuel separately, diesel fuel and liquefied petroleum gas, by using two mass flow meters *Krohne* type *Optimass 3050C* and *Optimass type 3300C*. The *Optimass 3050C* mass flow meter is used to determine the consumption of diesel fuel. The *Optimass 3300C* mass flow meter can be used to determine fluid flows in both liquid and gaseous states. The *Optimass 3300C* mass flow meter is used to determine the consumption of liquefied petroleum gas, being mounted between the evaporator and the gas tank, the liquefied petroleum gas being admitted in liquid state in the flow meter.

3.1.9. Data acquisition system

Measurement and recording of pressure in the engine cylinder and associated parameters it is carried out with a data acquisition system. From a constructive point of view, the data acquisition system consists of the following components: pressure transducer, charge amplifier, angular position transducer, data acquisition unit and PC computer equipped with acquisition plate.

The data acquisition system allows the recording of consecutive individual cycles and mediated cycles.

3.1.10. Equipment for measuring the level of pollutant emissions and greenhouse gases from exhaust gases.

AVL DiCom 4000 gas analyzer is used to measure the level of pollutant and greenhouse gases from diesel engine exhaust gases at the test bench at the test bench, which is equipped with an opacimeter for measuring the emission of smoke from exhaust gases [106].

The gas analyzer shall indicate the values measured in real time for the following parameters: air excess coefficient, level of the emissions of carbon monoxide, unburned hydrocarbons, carbon dioxide,

nitrogen oxides and oxygen, engine operating speed, oil temperature, the fuel injection timing (for compression ignition engine) and the spark timing (for the spark ignition engine) [106].

The emission of smoke from the exhaust gas is measured by a dynamic opacimeter indicating simultaneously the value of the exhaust gas opacity [%] and the smoke number $K [m^{-1}]$. The opacimeter measuring chamber is 0,215 [m] long and heated to 100 °C [106].

3.1.11. Organization of the experimental test bed

In order to study the operation of the diesel engine at the dual mode fuelling use, the experimental tests were carried out at the engine test bed, which consists of the equipment presented above. The scheme of the general organization of the test bed is shown in *figure 3.3.*:

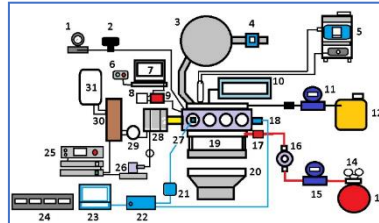


Fig. 3.3. Diagram of the experimental test bed. 1 – supercharge pressure indicator, 2 – bellows pressure gauge for measuring the supercharger pressure, 3 – air tank, 4 – flow meter for measuring air consumption, 5 – gas analyzer and opacimeter, 6 – LPG injector control, 7 – LPG fuelling system control computer, 8 – electronic control unit (UCE) of diesel engine K9K792, 9 – electronic control unit of LPG injectors (UG), 10 – engine cooling system, 11 – mass flow meter for diesel fuel, 12 – diesel fuel tank, 13 – LPG tank, 14 – pressure reducers, 15 – mass flow meter for LPG, 16 – LPG evaporator, 17 – LPG injector block, 18 – angular position transducer, 19 – K9K792 diesel engine, 20 – electric fan for cooling, 21 – charge amplifier, 22 – data acquisition unit *Indimodul 621*, 23 – computer of the data acquisition system, 24 – temperature indicators, 25 – dyno control panel and load control unit, 26 – actuator of load adjuster, 27 – piezoelectric pressure transducer, 28 – electric eddy-current dyno, 29 – dyno cooling system filter, 30 – dyno cooling system heat exchanger, 31 – dyno cooling system, 31 – water tank for the dyno cooling system.

3.1.12. Working procedure

For each investigated operating mode, the following were measured: condition parameters, effective power, engine torque, engine speed, air pressure and temperature in the engine inlet, exhaust gas temperature, coolant and oil temperature, hourly diesel consumption, hourly consumption of liquefied petroleum gas, hourly air consumption, level of pollutant emissions from exhaust gases (CO, HC, NO_x, exhaust gas opacity and smoke number K), CO₂ emission level. Using the data acquisition system, the variation in pressure in the engine cylinder is measured and recorded (indicated diagrams in $p-\alpha$ coordinates) being recorded for consecutive operating cycles. By processing the acquired data, the maximum pressure per cycle, the maximum pressure rise rate $(dp/d\alpha)_{max}$, the indicated mean effective pressure, the heat release rate, the moments per cycle when the conventional fractions of 5%, 10%, 50% and 90% of the heat release were released.

3.1.13. Diagnosis and repair of electric dyno HORIBA SCHENCK E90

Operation of the electric motor-dyno system

When commissioning the experimental test bed, it was found that the electric dyno cannot enter the working mode and does not allow the control of the operating regime of the engine, and for any mode of work chosen by the operator it is impossible to adjust the engine load and engine speed. **In the absence of adequate technical documentation for repair and / or maintenance operations, the difficulty of diagnosing the electric dyno is major**, the best solution in this case being that of understanding the operation of the electric dyno assembly - control actuator - control panel.

Diagnosis of the electric dyno-actuator system

The electric dyno-engine system starts but does not respond to the controls, and it is not possible to change the functional regime of the engine (load and speed). In order to verify the system, all the components such as: electric dyno, electric dyno power unit, electric dyno control unit, actuator of the accelerator pedal, power unit of the actuator, integrity and continuity of the electrical connections between them were individually diagnosed.

Diagnosis of electric dyno and electric dyno power unit

All electrical connections connecting the electric dyno to the power unit controlling the dyno were measured. Thus, the integrity of the two ring coils in the dyno stator and their operation were established, without the need for repair or maintenance operations.

Diagnosis of the actuator and the power unit of the actuator

The actuator shall not respond to any control sent by the operator from the dyno control panel and there is no error message or fault code displayed for the operator so that a particular technical problem can be identified.

Diagnostics of the electric dyno control panel unit

For no possible mode of work (constant load, constant speed) the control imposed by the operator from the control panel shall not be transmitted further to the electric dyno and the actuator of the accelerator pedal.

Electronic integrated circuit board for actuating the actuator. Diagnosis and repair.

Diagnosis: The difficulty of the stage is given by the lack of technical specifications and an electrical scheme for the integrated circuit board.

Since the integrity of the electrical circuits of the brake and its power unit had previously been verified, it was established that a possible defect would be present in the second *A100KDI* integrated circuit board interposed between the brake control panel and the electrical circuit of the brake stator.

Electronic integrated circuit board for operating the electric dyno. Diagnosis and repair.

Diagnosis: The difficulty of the stage is given by the lack of technical specifications and an electrical scheme for the integrated circuit board.

The fact that the electric brake does not produce a strong moment may cause a defect in the electronic integrated circuit board in the control circuit of the electric dyno.

Verification of the officials of the motor system - electric dyno

At partial load and low speed, the operation of the electric dyno was checked by measuring the parameters of interest, the electric input and output voltages for the control elements.

The electric dyno works according to the working characteristic, it can produce resistant moment in the range of 10...200 Nm.

Assembly and repositioning of equipment

For a better natural ventilation and static electrical insulation of the control equipment, it was resorted to modifying the laying systems by installing polyurethane supports with a height of 30 mm.

3.2. RESULTS OF THE EXPERIMENTAL INVESTIGATIONS

The experimental investigations were performed at stabilized operating modes, for engine loads of 40%, 55%, 70%, 85%, at speeds of 2000 rpm and 3900 rpm.

3.2.1. Determination of the degree of substitution of diesel fuel with liquefied petroleum gas

The diesel engine is fueled in a dual mode, and it is possible to operate only with diesel fuel or diesel fuel and liquefied petroleum gas, in different proportions, until the total substitution of diesel fuel. Starting the engine was carried out with the classic fuelling system. The degree of substitution is specified by the value of a coefficient called **the energy substitution coefficient**, which takes into account the lower heating value of the both fuels used.

3.2.2. Study of the influence of the degree of substitution on the specific energy consumption

At the 40% load and speed regime of 3900 rpm, compared to the diesel fuel supply, $x_c=0\%$, at the dual power supply, the brake specific consumption is reduced by a maximum of 3.5% for $x_c=8.14\%$, and for the use of higher degrees of substitution, the reduction of the brake specific consumption is of 1.88% for x_c maximum, *figure 3.16*. For degrees of substitution $x_c=20\%... 26\%$ of the brake specific consumption increases slightly by about 5.37%... 8.6%

In order to limit the variation in specific energy consumption by up to 3%, consideration may be given to limiting the degree of substitution to $x_c=20\%$, *figure 3.17*.

For the range $x_c=21.57\%... 36,23\%$ of the actual yield shall be reduced by 7%. At the maximum cyclical dose of LPG, $x_c=51,57\%$ the actual efficiency is kept in the range of operation at the classical fuelling, *figure 3.18*.

For dual fuelling, in the range $x_c=18\%... 32\%$ the brake specific consumption increases by 2.4%, and for $x_c=37\%... 43\%$ brake specific consumption is reduced by 0.6%... 1.2% vs. $x_c=18\%... 32\%$, an increase of a maximum of 2.1% to maximum x_c compared to the diesel fuel use, *figure 3.19*.

At this regime, the brake specific energy consumption increases by up to 3.6% at the degree of substitution $x_c=50\%$. Only in the range $x_c=32\%... 43\%$ increase is a maximum of 4.6%, *figure 3.20*. Thus, the effective efficiency is reduced by a maximum of 2% for the dual fuelling, when using small LPG cyclic doses, but the subsequent increase in the cyclic amount of LPG ensures the restoration of the effective efficiency to values similar to the operation of the diesel fuel fuelling, the difference being only 0.3% compared to the classic supply, *figure 3.21*.

At the 70% load and 3900 rpm speed regime there is a continuous improvement in engine economy, the brake specific consumption decreasing at the dual fuelling, especially at all degrees of substitution higher than $x_c=20\%$, compared to the classic fuelling, *figure 3.22*. For low degrees of

substitution, the brake specific consumption is 0.6...0.7% higher than the diesel supply, but when the amount of LPG in the cylinder increases, the brake specific consumption begins to decrease by 0.7% at $x_c=38\%$, by 0.44% at $x_c=44\%$ and by 4.5% at $x_c=51\%$, the economy of the engine being improved, *figure 3.22*.

In the case of dual fuelling, at the maximum degree of substitution, the brake specific energy consumption is reduced by 1.4%. For the value range of $x_c=15\%... 38\%$, the brake specific energy consumption does not exceed by 2.1% the value allocated to $x_c=0\%$, *figure 3.23*.

The brake efficiency, *figure 3.24*, begins to increase with the increase in the cyclic amount of LPG, when x_c exceeds values of 0.3%. For dual fuelling, where the degree of substitution varies in the range of $x_c=38\%... 51\%$, the effective efficiency increases by up to 4.8% compared to the diesel fuel supply. Compared to the classical fuelling, $x_c=0\%$, in the dual feed the brake efficiency increases by 0.6% at $x_c=38\%$, by 2.4% at $x_c=44\%$ and by 4.8% at $x_c=51\%$, [19]. Similar information was also presented in works [107], [108].

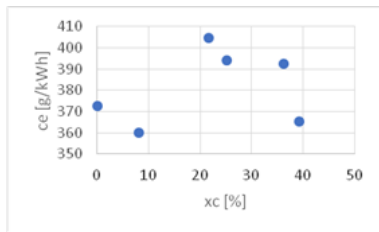


Fig. 3.16 Brake specific consumption for varying degrees of substitution at 40% partial load and 3900 rpm

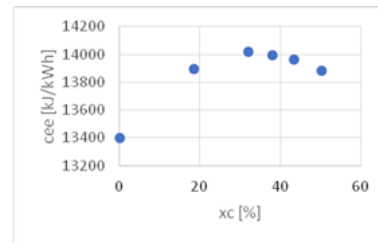


Fig. 3.20 Brake specific energy consumption for varying degrees of substitution at 55% partial load and 3900 rpm

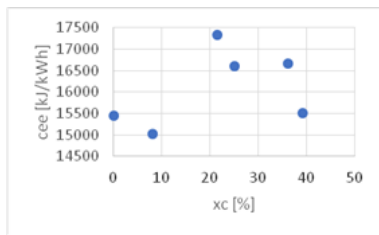


Fig. 3.17. Brake specific energy consumption for varying degrees of substitution at 40% partial load and 3900 rpm

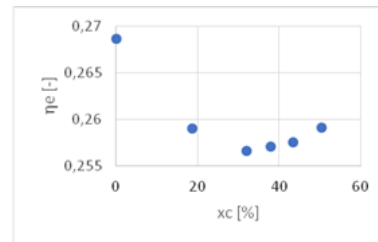


Fig. 3.21 Effective efficiency for varying degrees of substitution at 55% partial load regime and 3900 rpm speed

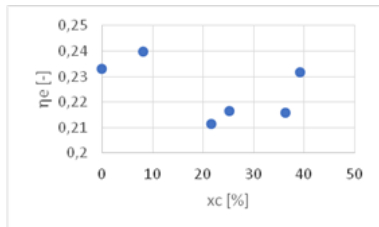


Fig. 3.18. Effective efficiency for varying degrees of substitution at 40% partial load regime and 3900 rpm

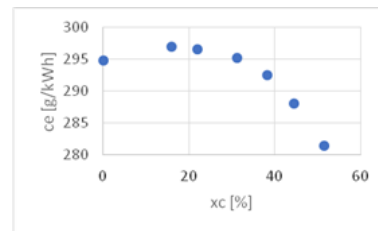


Fig. 3.22 Brake specific consumption for varying degrees of substitution at 70% partial load regime and 3900 rpm

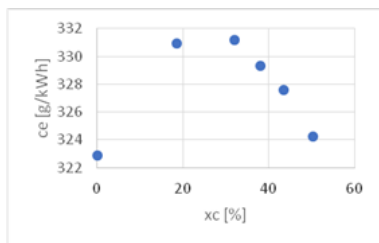


Fig. 3.19. Brake specific consumption for varying degrees of substitution at 55% partial load regime and 3900 rpm

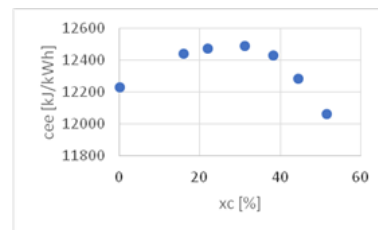


Fig. 3.23 Brake specific energy consumption for varying degrees of substitution at 70% partial load and 3900 rpm

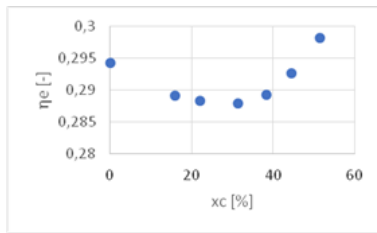


Fig. 3.24. Effective efficiency for varying degrees of substitution at 70% partial load regime and 3900 rpm

3.2.3. Study of the influence of the degree of substitution on the mechanical stresses of the engine. Maximum pressure. Maximum pressure rise rate

At the 40 % part-load and 3900 rpm speed, *figure 3.25*, at the diesel and LPG fuelling in general, the maximum pressure does not far exceed the values recorded for the diesel fuel use. At $x_c = 21.57\%$ the maximum pressure increases by 1.9% compared to the classical fuel use, but the values recorded also in the individual cycles do not exceed the usual allowable values, the reliability of the engine being preserved also at the dual fuelling. The angle of maximum pressure tends to approach the TDC (Top Dead Centre), with the maximum cycle pressure being reached later with the increase in the cyclic dose of LPG, *figure 3.26*.

The maximum pressure rise rate, *figure 3.27*, tends to increase with the increase in the LPG dose, from 1.88 bar/CAD to $x_c=0\%$ to 3.26 bar/CAD at $x_c=36.23\%$ (CAD-crank angle degree).

At the 55% load regime, the maximum cycle pressure increases by a maximum of 7.6% to the diesel fuel and LPG fuelling for the maximum degree of substitution, *figure 3.28*.

With the increase in the degree of substitution, the angle at which the maximum pressure occurs tends to depart from the value allocated to diesel fuel operation, *figure 3.29*.

The maximum pressure rise rate, *figure 3.30*, has moderate values compared to the growth trend from the 40% load regime, in line with the fact that at the 55% load the cyclic doses of LPG are much lower, the maximum pressure increase speed not exceeding 5.91 bar/CAD, which is 61% higher than the value recorded in the diesel-only supply.

At 70% load, on diesel fuel and LPG fuelling, in the $x_c=38\%$ range... 51%, the maximum pressure increases by 5.2%... 11,7 % compared to the value found at the classical fuel use, the values not exceeding the allowable range that ensures the normal operation of the engine, *figure 3.31*.

The angle of maximum pressure is reached later on the cycle in the case of the dual supply in general, *figure 3.32*, but at certain degrees of substitution $x_c=15\%$ or $x_c=38\%$, the maximum pressure angle tends to approach the TDC or to be kept within the range of values allocated to diesel fuel operation.

In the case of dual fuelling, for degrees of substitution of up to $x_c=31\%$, the values for the maximum speed of pressure increase are maintained in the range of the value found in the classical supply, $x_c=0\%$. When increasing the degree of substitution $x_c= 38\%... 51\%$ also increases the maximum rate of pressure increase, reaching values with 71%, 102% and 156% higher than the classic supply, at $x_c= 38\%$, 44% and 51%, respectively, *figure 3.33*.

The upward trend recorded for maximum pressure and the maximum rate of pressure increase with the increase of the cyclic dose of LPG may be a criterion for limiting the value of x_c , to all investigated operating regimes, [109], [110], [111].

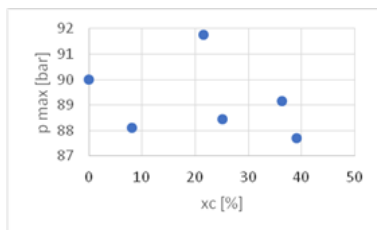


Fig. 3.25 Maximum pressure for varying degrees of substitution at 40% partial load regime and 3900 rpm

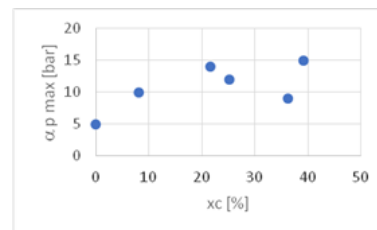


Fig. 3.26 Maximum pressure angle for varying degrees of substitution at 40% partial load and 3900 rpm speed

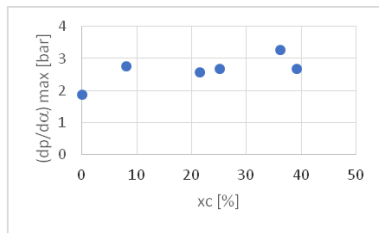


Fig. 3.27 Maximum pressure increase speed for varying degrees of substitution at 40% partial load regime and 3900 rpm

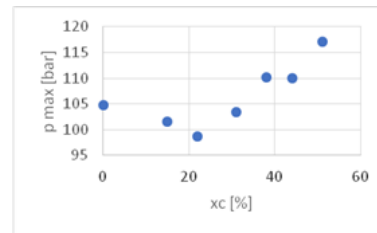


Fig. 3.31 Maximum pressure for varying degrees of substitution at 70% partial load and speed 3900 rpm

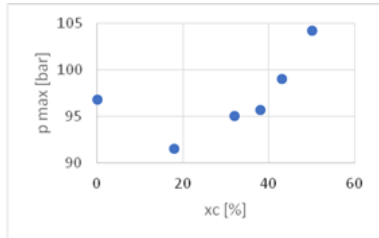


Fig. 3.28 Maximum pressure for varying degrees of substitution at 55% partial load regime and speed 3900 rpm

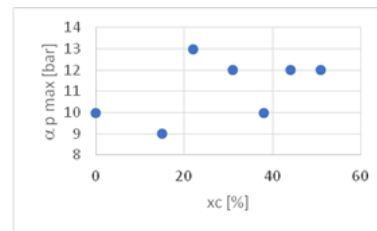


Fig. 3.32 Maximum pressure angle for varying degrees of substitution at 70% partial load regime and speed 3900 rpm

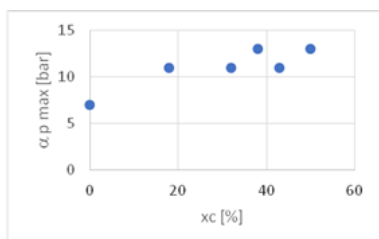


Fig. 3.29 Maximum pressure angle for varying degrees of substitution at 55% partial load regime and 3900 rpm

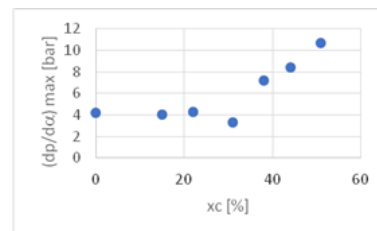


Fig. 3.33 Maximum pressure increase speed for varying degrees of substitution at 70% partial load regime and 3900 rpm

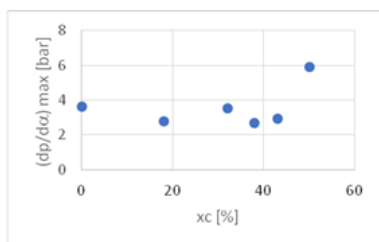


Fig. 3.30 Maximum pressure increase speed for varying degrees of substitution at 55% partial load regime and 3900 rpm

3.2.4. Study of the influence of the degree of substitution on the level of polluting emissions of the diesel engine of a car powered by liquefied petroleum gas

At partial load 40% and speed of 3900 rpm, *figure 3.39*, the NO_x emission level is reduced by a maximum of 29% at $x_c=21.57\%$. And at the other degrees of substitution the NO_x emission level is reduced by up to 21,5% compared to the NO_x emission level measured when the engine is operated on the diesel supply. At 55% load and 3900 rpm, *figure 3.40*, at dual fuelling the NO_x emission level is continuously reduced by up to 17.7% to x_c maximum compared to $x_c=0\%$. At 70% load and 3900 rpm, *figure 3.41*, the NO_x emission level is continuously reduced by up to 22.3% when the degree of substitution increases.

At the 3900 rpm speed regime, high-speed combustion of homogeneous air-LPG mixtures ensures a reduction of HC emission level by up to 52.5% at 40% load, *figure 3.42*, by up to 85.7% at 55% load, *figure 3.43* and by 98.3% at 70% load, *figure 3.44*, respectively.

The emission of smoke from the exhaust gases is assessed by the opacity and smoke number K measured at the speed regime of 3900 rpm, at loads of 40%, 55% and 70%, *figures 3.45...3.50*. At the 40% load regime, the opacity is reduced by up to 67.5%, at $x_c=21.57\%$ compared to the classical fuelling, the reduction being important, of 62.5% and to the maximum degree of substitution, $x_c=39.14\%$, *figure 3.45*.

The smoke number K, *figure 3.46*, is reduced by up to 66.6% on dual fueling and maximum degree of substitution compared to the diesel fuel fuelling, with more significant reductions being recorded as early as the range $x_c=21.57\%... 39.41\%$ of the degree of substitution.

At the dual fuelling, at the 55% load regime, the level of exhaust gas opacity is reduced by 50% ($x_c=50\%$) compared to the classical fuelling, *figure 3.47*. and the smoke number K is reduced by 55.5% at the dual fuelling for the maximum degree of substitution, *figure 3.48*.

At the 70% load regime, compared to the classic fuelling, at the engine fuelled with diesel fuel and LPG a continuous reduction appears for the exhaust gas opacity level by up to 39.13% at $x_c=50\%$, the reductions being more significant after $x_c=30\%$, in the range $x_c=31\% \dots 51\%$, *figure 3.49*. The smoke number K, *figure 3.50*, is reduced by up to 45.4% at the dual fuelling, from $x_c=31\%$ the reduction of the smoke number being more important compared to the lower degrees of substitution.

A continuous reduction in the level of carbon dioxide emissions is observed in all investigated load regimes investigated. The level of CO₂ emission is reduced by 9.4% at the 40% load regime, *figure 3.51*, by 3.1% at the 55% load regime, *figure 3.52* and by 6.58% at the 70% load regime, *figure 3.53* reduction being related to the maximum degree of substitution used in that regime.

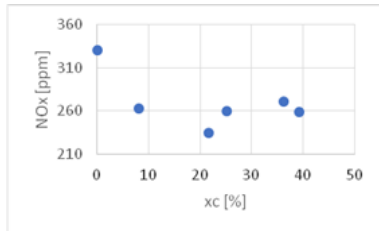


Fig. 3.39. Variation of NO_x emission level with the degree of substitution at load 40% and speed of 3900 rpm

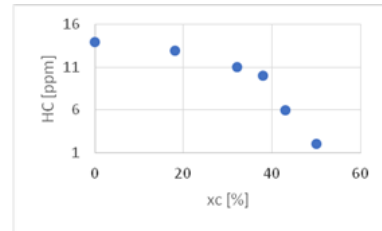


Fig. 3.43. Variation in HC emission level with degree of substitution at 55% load replacement and speed of 3900 rpm

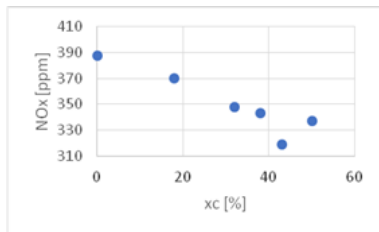


Fig. 3.40. Variation of NO_x emission level with the degree of substitution at load 55% and speed of 3900 rpm

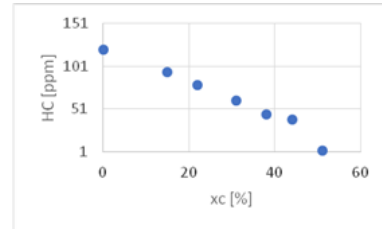


Fig. 3.44. Variation in HC emission level with degree of substitution at 70% load substitution rate and speed of 3900 rpm

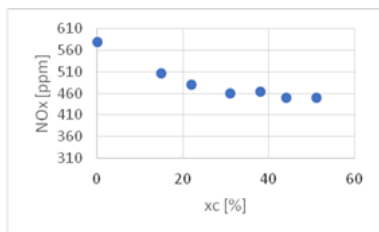


Fig.3.41. Variation of NO_x emission level with the degree of substitution at load 70% and speed of 3900 rpm

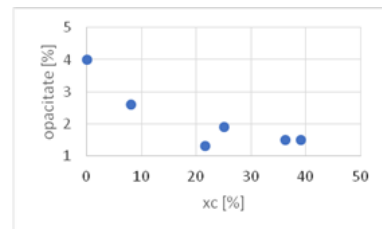


Fig.3.45. Variation of smoke emission level (assessed by the opacity value) with the degree of substitution at load 40% and speed of 3900 rpm

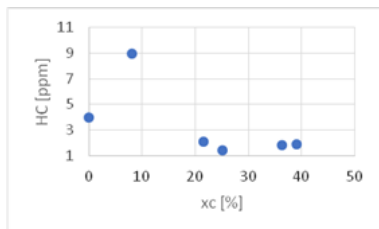


Fig. 3.42 Variation of HC emission level with the degree of substitution at 40% load and speed of 3900 rpm

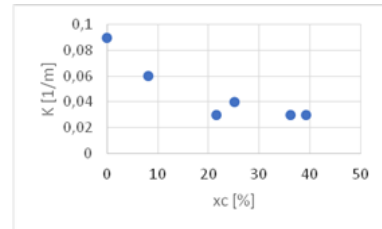


Fig.3.46. Variation of smoke emission (assessed by the K smoke number) with the degree of substitution at 40% load and speed of 3900 rpm

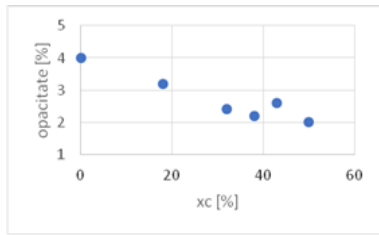


Fig. 3.47. Variation of smoke emission (assessed by the opacity value) with the degree of substitution at load 55% and speed of 3900 rpm

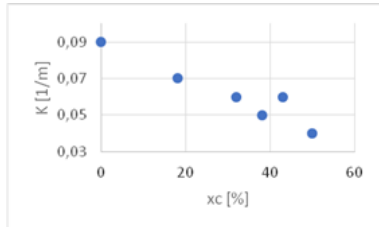


Fig. 3.48 Variation of smoke emission (assessed by smoke number K) with the degree of substitution at load 55% and speed of 3900 rpm

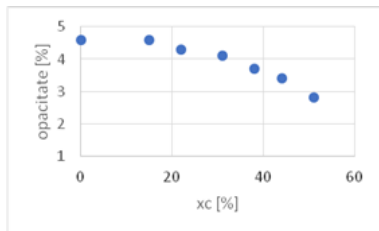


Fig. 3.49 Variation of smoke emission (assessed by the opacity value) with the degree of substitution at load 70% and speed of 3900 rpm

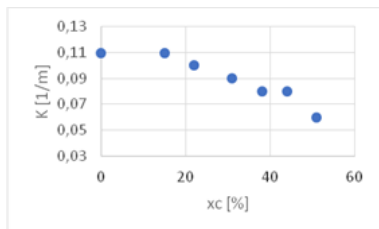


Fig. 3.50 Variation of smoke emission (as assessed by the K smoke number) with the degree of substitution at load 70% and speed of 3900 rpm

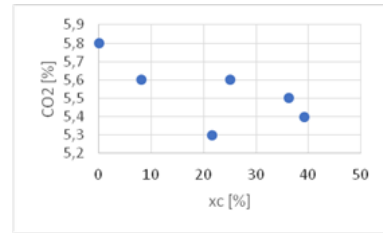


Fig. 3.51 Variation in CO₂ emission level with the degree of substitution at 40% load and speed of 3900 rpm

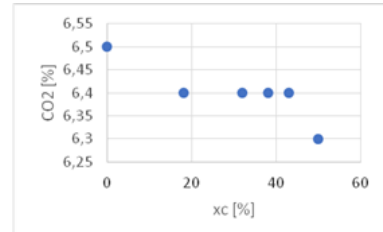


Fig. 3.52 Variation in CO₂ emission level with the degree of substitution at 55% load and speed of 3900 rpm

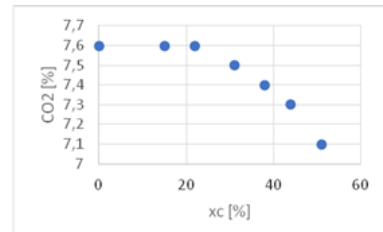


Fig. 3.53. Variation in CO₂ emission level with degree of substitution at 70% load and speed of 3900 rpm

3.2.5. Study of the influence of the degree of substitution on the cyclic variability of the combustion process in the car diesel engine fuelled with liquefied petroleum gas

The coefficient $(COV)_{p_{max}}$ does not exceed 1,44 %, but for the range $x_c = 6,7 \% \dots 28\%$, there is a clear upward trend, the value calculated for $x_c=28\%$ being ~ 2.5 times higher than that of the standard engine, *figure 3.54*.

Compared to the exclusive diesel fuel supply, the coefficient $(COV)_{IMEP}$ for the indicated mean effective pressure (IMEP) increases by 1.2 times to the maximum degree of substitution, *figure 3.55*, the cyclic variability of the flame development at the beginning of combustion not being significantly influenced by the increase in the degree of substitution.

The variability of the maximum pressure angle is kept at the same intensity at the dual power supply as in the case of the classical power supply, *figure 3.56*, for small degrees of substitution, $x_c = 2.5\%$, the value of $(COV)_{\alpha_{p_{max}}}$ is lower compared to the value recorded in the classic engine.

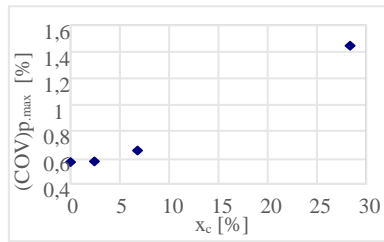


Fig. 3.54. Coefficient $(COV)_{p_{max}}$ at varying degrees of substitution x_c at speed 2000 rpm and 85% load

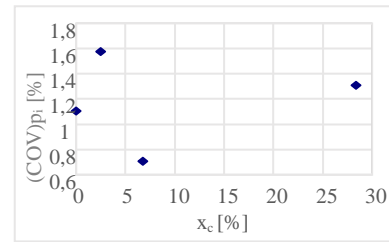


Fig. 3.55. Coefficient $(COV)_{IMEP}$ at varying degrees of substitution x_c at speed 2000 rpm and 85% load.

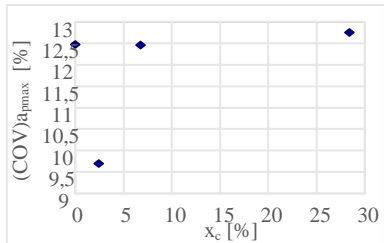


Fig. 3.56. Coefficient $(COV)_{\alpha_{pmax}}$ at varying degrees of substitution x_c at speed 2000 rpm and 85% load

The increase in the maximum pressure and the maximum pressure rise rate at the dual fuelling correlates with the tendency to bring the maximum pressure angle closer to the TDC, which indicates a rapid, more brutal combustion compared to the situation of the diesel fuel use, *figure 3.57*. The values for the angle at which the maximum pressure in the mediated cycles (indicatively "average") occurs are presented in comparison with the minimum and maximum values, indicative "minimum" and "maximum", respectively, found in the individual cycles used in mediation.

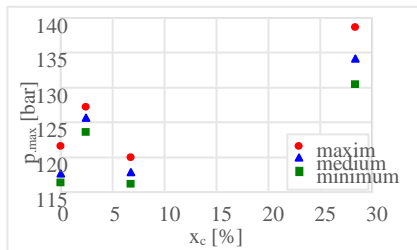


Fig. 3.57 Cyclic dispersion between maximum pressure values at varying degrees of substitution x_c at speed 2000 rpm and 85% load.

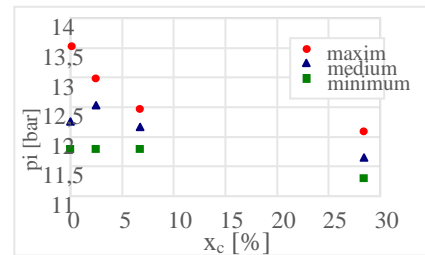


Fig. 3.59 Cyclic dispersion between the average pressure values indicated at varying degrees of substitution x_c at speed 2000 rpm and 85% load.

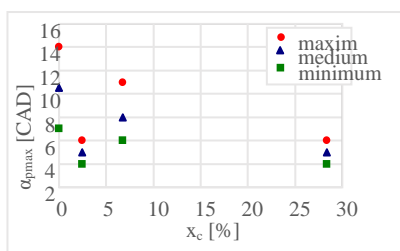


Fig. 3.58 Cyclic dispersion between the values of the maximum pressure angle at varying degrees of substitution x_c at speed 2000 rpm and 85% load.

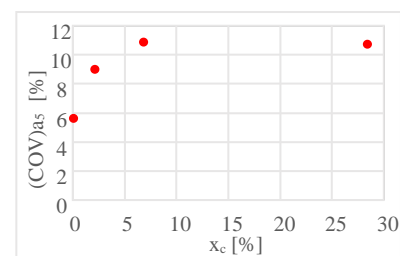


Fig. 3.60. Variation coefficient $(COV)_{\alpha_5}$ at varying degrees of substitution x_c at speed 2000 rpm and 85% load.

In the case of diesel fuel and LPG fuelling, there is a tendency to amplify the variability of the combustion process at the increase of the LPG dose, expressed by the variability of the angles α_5 , α_{10} , α_{50} and α_{90} , which establish the moments when 5%, 10%, 50% and 90% of the heat are released. The ultra-lean air-LPG mixtures established in the cylinder before the start of combustion influence the cyclic variability of the beginning of combustion, evaluated by the variability of the angle of 5% of the heat release. The value of $(COV)_{\alpha_5}$ increases from 5.6%, in the case of the classic power solution, to 10.7%... 11% for higher substitution rates, *figure 3.60*. The COV coefficient for the 10% MFB (mass fraction burned), *figure 3.61*, increases from 6.6% to 106% at the maximum degree of substitution as a result of the combustion of ultra-lean air-LPG mixtures.

As a result of the high combustion rates of air-LPG mixtures, the acceleration of the combustion process leads to the acceleration of the heat release process, the increase in the rate of heat release and

the earlier reaching of the 50 and 90 % of the heat released, respectively, on the cycle, compared to diesel fuel, the dispersion between the cyclic values of the α_{50} % being lower, *figure 3.62*.

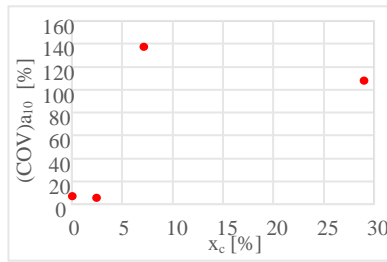


Fig. 3.61 Variation coefficient (COV) α_{10} at different degrees of substitution x_c at speed 2000 rpm and 85% load.

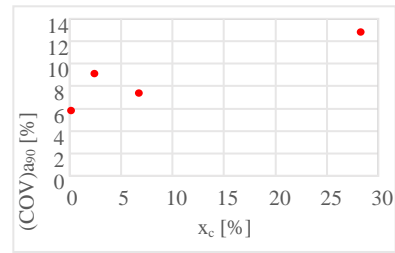


Fig. 3.63 The coefficient variation (COV) α_{90} at different degrees of substitution x_c at speed 2000 rpm and 85% load.

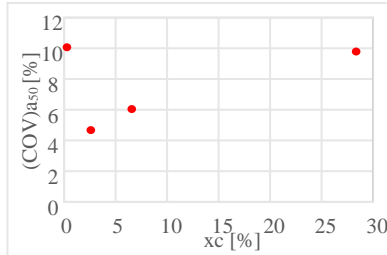


Fig. 3.62 Coefficient variation (COV) α_{50} at varying degrees of substitution x_c at 2000 rpm and 85% load.

At the LPG use, the higher cyclic variability at the beginning of combustion, expressed by the values of the coefficients (COV) $\alpha_{5\%}$, (COV) $\alpha_{10\%}$, leads to an increased cyclic variability for the end of combustion, as determined by the cyclic variability of the time of reaching 90 % MFB, *figure 3.63*.

Even if the maximum value does not exceed 1.76%, without the need to limit x_c to this regime and according to this criterion, the trend of increasing (COV) p_{max} with the increase x_c , especially for $x_c > 10\%$, can be taken into account, *figure 3.64*.

At the 70% load regime, (COV) p_{max} at $x_c = 12\%$ is 2.47 times higher than the value allocated to the exclusive diesel fuel supply. The maximum calculated value does not exceed 1.72%, but also at this load regime there is a tendency to increase the values (COV) p_{max} with the degree of substitution, especially for $x_c > 9\%$, *figure 3.64* and *figure 3.65*. In this load regime, the angle of maximum pressure, $\alpha_{p_{max}}$, tends to approach PMI, which characterizes a faster, more "brutal" combustion process. The cyclic variability of the $\alpha_{p_{max}}$ tends to increase slightly to x_c maximum, *figure 3.66* and *figure 3.67*, compared to the reference regime, $x_c = 0\%$. At 55% load, for $x_c = 1.2\% \dots 19\%$ its values (COV) $\alpha_{p_{max}}$ increase to 23%... 74% in dual power, which also signifies an increase in cyclic variability at the beginning of combustion.

For the speed of 2000 rpm, the values of (COV) $IMEP$ are two times higher for all degrees of substitution than the diesel fuel use and 55% load, *figure 3.68* and *figure 3.69*. At 70% load, the values for (COV) $IMEP$ increase 1.5 times to the maximum degree of substitution. At both loads, 55% and 70%, the increase in the cyclic dose of LPG leads to an increase in the maximum pressure and dispersion between its values found in the individual cycles, *figures: 3.64; 3.65; 3.66; 3.67; 3.68; 3.69*. At $x_c = 9.6\% \dots 12\%$, the values of (COV) $IMEP$ increase by 1.7 times compared to the low degrees of substitution $x_c = 5.6\%$, *figure 3.68* and *figure 3.69*. The values determined for COV of maximum pressure and mean pressure indicated shall not, however, exceed the maximum allowable value of 10 % [114].

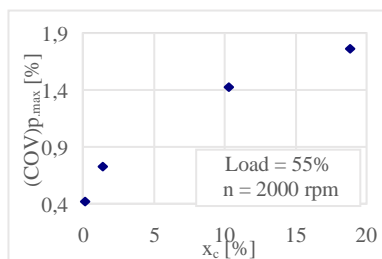


Fig. 3.64 Coefficient (COV) p_{max} at varying degrees of substitution x_c at speed 2000 rpm and load 55%.

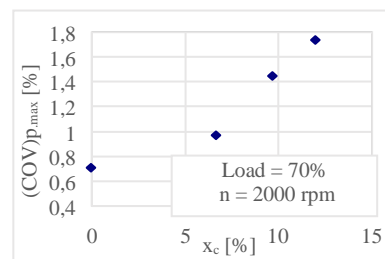


Fig. 3.65 Coefficient (COV) p_{max} at varying degrees of substitution x_c at speed 2000 rpm and load 70%.

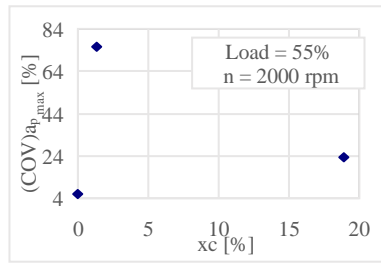


Fig. 3.66 The coefficient (COV) $\alpha_{p_{max}}$ at varying degrees of substitution x_c at speed 2000 rpm and load 55%."

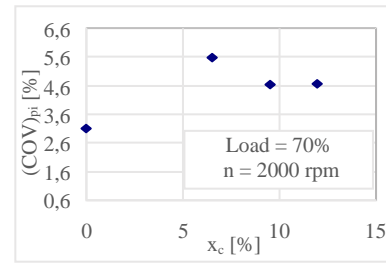


Fig. 3.69 Coefficient (COV) IMEP at varying degrees of substitution x_c at speed 2000 rpm and load 70 %.

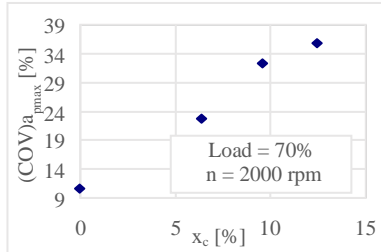


Fig. 3.67 The coefficient (COV) $\alpha_{p_{max}}$ at varying degrees of substitution x_c at speed 2000 rpm and load 70 %.

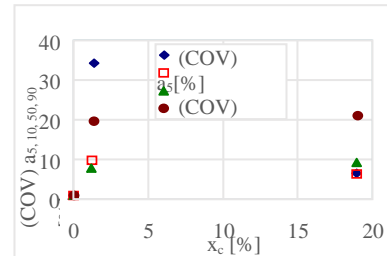


Fig. 3.70. The coefficient variation (COV) α_5 , (COV) α_{10} , (COV) α_{50} and (COV) α_{90} at varying degrees of substitution x_c at speed 2000 rpm and load 55%.

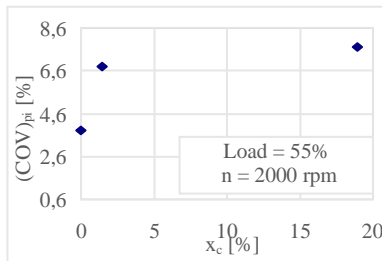


Fig. 3.68 Coefficient (COV) IMEP at different degrees of substitution x_c at speed 2000 rpm and load 55 %.

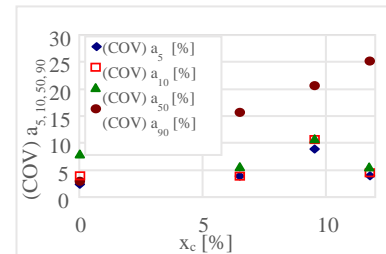


Fig. 3.71 Coefficient variation (COV) α_5 , (COV) α_{10} , (COV) α_{50} and (COV) α_{90} at varying degrees of substitution x_c at speed 2000 rpm and load 70%.

Compared to the diesel fuel use, at the dual fuelling, the beginning of combustion is characterized by higher cyclic variability, the value of $(COV)\alpha_{5\%}$, increasing 6.15 times at the load of 55% and 1.7 times at load of 70%, *figure 3.70* and *figure 3.71*. The end of the combustion process is characterized by a higher cyclic variability, at the dual fuelling the value of $(COV)\alpha_{90\%}$ increasing by 24.5 times at the load of 55% and about 8 times for the load of 70%, compared to $x_c=0\%$, *figure 3.70* and *figure 3.71*.

Figure 3.72 shows the variation in the maximum pressure for 300 consecutive cycles, for the diesel fuel use ($x_c=0\%$) and for the dual fuelling, with diesel fuel and liquefied petroleum gas, for the maximum cyclic dose of LPG ($x_c=51.57\%$).

The cyclic dispersion of the maximum pressure begins to increase slightly for the degrees of substitution $x_c=25.11\% \dots 51.57\%$ as shown in *figure 3.72* and *figure 3.73*. The coefficient of variability of the maximum pressure $(COV)p_{max}$ does not exceed the value of 2,28% for $x_c = 51,57\%$. For values of COV not exceeding 10% it is considered that the normal operation of the engine is ensured.

A similar trend of COV variation for the indicated mean pressure, *figure 3.74*, is recorded. In dual fuelling, $(COV)_{imep}$ increases from 0.59%, for diesel fuelling, to 0.98% for $x_c=51.57\%$.

For LPG and diesel fuel use, the 5% MFB appears later on the cycle, compared to the classic fuelling, the angle of 5% MFB being about 1 CAD farther from the TDC, the range of variation being 0,5 to 1,5 CAD, *figure 3.75*.

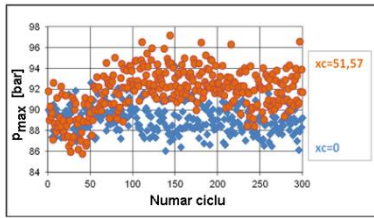


Fig. 3.72. Dispersion between the maximum pressure values for the diesel fuelling ($x_c=0\%$) and diesel fuel and LPG ($x_c=51.57\%$), at the 40% load and speed regime 3900 rpm

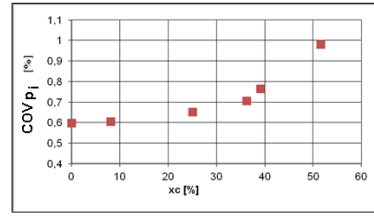


Fig. 3.74 COV coefficient for the average pressure indicated at different degrees of substitution x_c , at the 40 % load regime and speed 3900 rpm

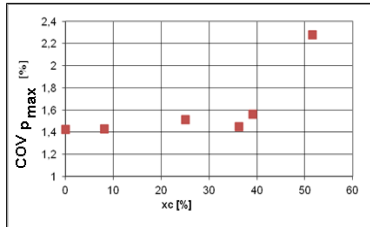


Fig. 3.73 COV coefficient for maximum pressure at different degrees of substitution x_c , at 40 % load and speed 3900 rpm

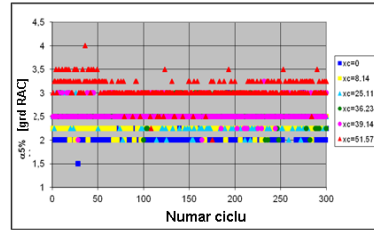


Fig. 3.75 Corresponding angle 5% MFB at different degrees of substitution x_c , at 40% load and speed 3900 rpm

The first stage of heat release is achieved much later on the operating cycle, for all degrees of substitution x_c , but the cyclic dispersion between the angle values of 5% MFB is slightly reduced by increasing the cyclic dose of LPG, the COV for 5%-MFB decreasing from 8.16% ($x_c=0\%$) to 7.02% ($x_c=51.57\%$), *figure 3.76*. At the dual fuelling, in some individual cycles, the MFB of 5% is reached at the same angle intervals as at the diesel fuel use.

For 10% MFB, a similar trend of variation is maintained, so with the increase in the degree of substitution, the value of $\alpha_{10\%}$ begins to move away from the TDC, with values in the range of 1...1.5 degrees, *figure 3.77*, but also for the diesel fuel use, in a few individual cycles 10% MFB is reached at similar times on the cycle as at the dual fuelling use, for all degrees of substitution.

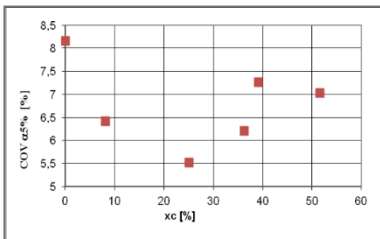


Fig. 3.76 Value of the COV coefficient for $\alpha_{5\%}$ at different degrees of substitution x_c , at the regime of 40% load and speed of 3900 rpm

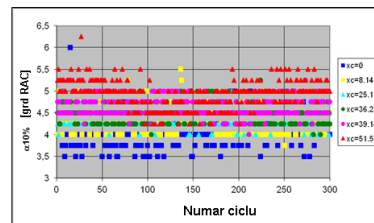


Fig. 3.77 Corresponding angle 10% MFB at different degrees of substitution x_c , at 40% load and speed of 3900 rpm

The decrease in the cyclic dose of diesel fuel, with the increase in the amount of LPG, leads to reaching later per cycle the percentages of 5% and 10% of the reaction heat. Also, in this case the cyclic dispersion between these values is subtracted at the increase of x_c , $(COV)\alpha_{10\%}$ decreases from 8.7% ($x_c=0\%$) to 6.46% at x_c maximum, *figure 3.78*.

Values for $\alpha_{COV 50\%}$ and $(COV)\alpha_{90\%}$ start to increase for $x_c=36.23\% \dots 51.57\%$, but do not exceed the allowable value of 10%, *figure 3.80* and *figure 3.82*.

The value for the coefficient $(COV)\alpha_{50\%}$ increases from 2.61% ($x_c=0\%$) to 3.69% ($x_c=51.57\%$), *figure 3.81*, and the value for $(COV)\alpha_{90\%}$ increases from 5.04% to 9.58% at the maximum degree of substitution, *figure 3.83*.

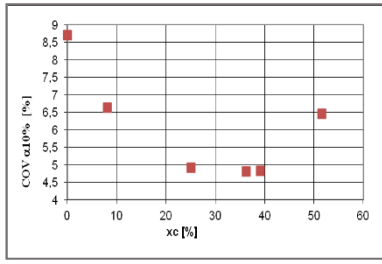


Fig. 3.78 Value of the COV coefficient for $\alpha_{10\%}$ at different degrees of substitution x_c , at the 40% load and speed regime 3900 rpm

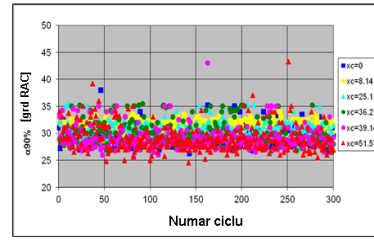


Fig. 3.81 Corresponding angle 90% MFB at different degrees of substitution x_c , at 40% load and speed of 3900 rpm

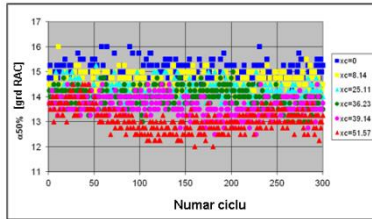


Fig. 3.79 Corresponding angle 50% MFB at different degrees of substitution x_c , at 40% load and speed of 3900 rpm

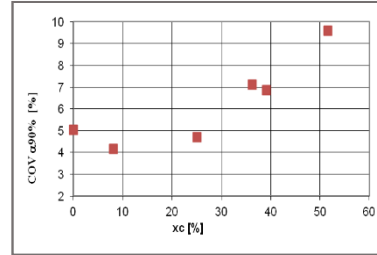


Fig. 3.82 Value of the COV coefficient for $\alpha_{90\%}$ at different degrees of substitution x_c , at the 40% load regime and speed of 3900 rpm

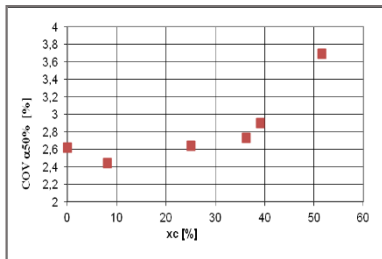


Fig. 3.80 Value of the COV coefficient for $\alpha_{50\%}$ at different degrees of substitution x_c , at the 40% load and speed regime 3900 rpm

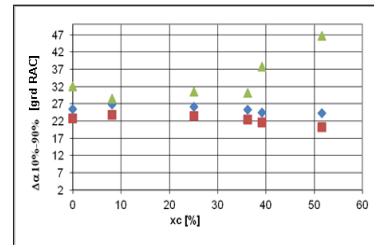


Fig. 3.83 The trend of variation in the combustion duration $\Delta\alpha_{10\%-90\%}$ for different degrees of substitution x_c , as determined by its minimum (in red), average (in blue) and maximum (in green) values from the individual cycles, at the regime of 40% load and speed 3900 rpm

The general tendency to increase the cyclic variability of combustion at the LPG use is reflected by the values of the coefficients of cyclic variability determined for the maximum pressure, the indicated mean effective pressure, the moments when 50% and 90% of the reaction heat is released, values that increase with the increase of the cyclic dose of LPG, but without exceeding the allowable value of 10%.

3.3. CONCLUSIONS OF THE EXPERIMENTAL INVESTIGATIONS

The main conclusions of the experimental investigations of the car diesel engine fuelled with liquefied petroleum gas are as follows: *the brake specific consumption is reduced by a maximum of 3.5% to the 40% load regime, increases by 2.4% at the 55% load regime and is reduced by up to 4.5% to the 70% load regime. The brake specific energy consumption is reduced by 2.86% at the 40% load and by 1.4% at the 70% load. As the influences of the degree of substitution depend on the load regime, the value of the degree of substitution x_c used may be limited due to the limitation of the worsening of the engine economy to the increase of the cyclic dose of LPG and the maintenance of the actual efficiency in the range of the usual values; the tendency to increase the maximum pressure values and the maximum pressure rise rate with the increase of the cyclic dose of LPG, the upward trend which may be limited by limiting the value of x_c to all operating modes investigated; the level of NOx emission decreases by 42% due to the reduction of the amount of available oxygen and the reduction of the gas temperature when increasing the degree of substitution of diesel fuel with LPG, at the regime of 85% load and speed 2000 rpm; at partial load 40% and speed 3900 rpm, the level of NOx emission is reduced by a maximum of 29% to $x_c = 21.57\%$. At the other degrees of substitution, the NOx emission level is reduced by up to 21,5 % compared to the NOx emission level measured when the engine is operated on the diesel supply. At 55% load and 3900 rpm speed, at dual power supply the NOx emission level is continuously reduced by up to 17.7% to x_c maximum compared to $x_c = 0\%$. At 70% load and 3900 rpm, the NOx emission level is continuously reduced by up to 22.3% when increasing substitution. The reduction in the level of nitrogen oxides can be explained by the reduction of the oxygen available in the cylinder with the increase in the dose of LPG injected into the engine intake and by the acceleration of the combustion*

process when the homogeneous air-LPG mixtures are burned at a higher speed, by reducing the time available for the formation of nitrogen oxides.

The values calculated for the coefficients of cyclic variability for the maximum pressure, the indicated average pressure and for the angles $\alpha_5\%$, $\alpha_{10}\%$, $\alpha_{50}\%$ and $\alpha_{90}\%$ do not exceed the permissible limit of 10 %, which indicates that the normal operation of the diesel engine is also ensured for the dual diesel fuel and LPG fuelling, using a degree of substitution of up to $x_c = 51,57\%$.

CHAPTER IV

4. MODELING OF THERMOGASODYNAMIC PROCESSES IN THE CYLINDER OF THE DIESEL ENGINE FUELLED WITH LPG

For the simulation of thermo-gas-dynamic processes in the engine cylinder, physic-mathematical models elaborated on the basis of hypotheses are used. The author simulated the thermo-gas-dynamic processes in the cylinder of the engine with a zero-dimensional physic-mathematical model that he developed, a model called **MUSA** (One zone Model for Combustion Study).

In order to deepen the analysis of the influences of the degree of substitution of diesel fuel with LPG on the operation of the diesel engine when dual-mode diesel fuel and LPG fuelling, the author has developed a one-zone thermodynamic model for the study of vaporization, mixture formation and combustion of diesel droplet, a model called by the author **SVAP** (Study of Vaporization and Combustion of diesel fuel drop). To this physic-mathematical model attached sub-models for simulating the formation and combustion of soot and the formation of nitrogen monoxide.

4.1. MODELING OF THERMOGASODYNAMIC PROCESSES IN THE ENGINE CYLINDER - MUSA MODEL

4.1.1. Assumptions

The gas mixture is considered chemically and thermally homogeneous. It is considered that the gas mixture has the properties of the perfect gases. The flow of gases in the exhaust and intake shall be considered at all times. The flow of gases through the holes controlled by the valves is considered adiabatic. The internal energy and enthalpy of gases is determined using real specific heat, considering mixtures of gases, [9], [114], [116], [117].

4.1.2. Gas exchange processes

The calculation of gas exchange processes requires knowledge of the state parameters of the gases inside the cylinder at the opening of the exhaust valve evaluated in advance by the approximate calculation of the engine cycle.

4.1.3. The compression process

The calculation of compression begins from the moment of closing the intake valve. The amount of gases inside the cylinder and their composition does not change during the compression process.

4.1.4. The combustion process

The firing process is simulated using formal double Vibe laws, [1].

4.1.5. The expansion process

The amount of gases inside the cylinder and their composition do not vary during the process of relaxation. The calculation of expansion is carried out until the moment of opening the exhaust valve.

4.1.6. The results of the simulation of thermo-gas-dynamic processes

The degree of substitution of diesel fuel with LPG is specified by the value of **the energy substitution coefficient**, x_c , as defined in Chapter 3. *Figure 4.2* shows the combustion laws for different values of the substitution coefficient of diesel fuel with LPG.

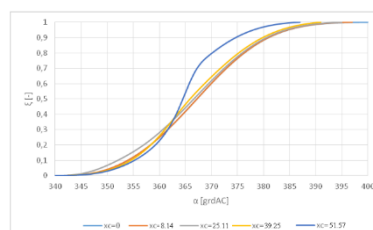


Fig. 4.2. Double Vibe law for different substitution values

Maximum pressure. Maximum temperature

Figures 4.3 to 4.7 show the variation in pressure and temperature inside the cylinder when standard and dual-mode fuelling engine operation.

In standard fuelling, $x_c=0\%$, the pressure in the cylinder reaches a maximum of 87,8 bar, at $\alpha=366$ CAD (1080 CAD is the equivalent of 360 CAD, and the temperature reaches a maximum of 1635 K, at 29 CAD after TDC, *figure 4.3*.

When dual-mode is used, at diesel fuel and LPG fuelling, for substitution ratio $x_c=8.14\%$, the in-cylinder pressure reaches a maximum of 87.1 bar at $\alpha=368$ CAD and the temperature reaches a maximum of 1710.6 K at 29 CAD after the TDC, *figure 4.4*.

At dual fuelling, for the degree of substitution $x_c=25.11\%$, the pressure in the cylinder reaches a maximum of 87 bar, at 6 CAD after TDC, and the temperature reaches a maximum of 1721.8 K, at 28 CAD after TDC, *figure 4.5*.

For the degree of substitution $x_c=39.25\%$, the in-cylinder pressure reaches a maximum of 85,8 bar, at 5 CAD after TDC, and the temperature reaches a maximum of 1781,3 K, at 29 CAD after TDC, *figure 4.6*.

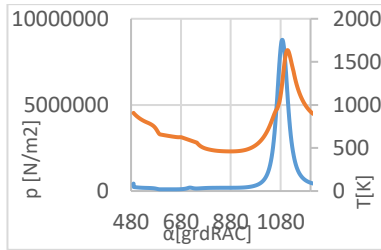


Fig. 4.3. Pressure and temperature inside the cylinder for the case of diesel fuel use, $x_c=0\%$.

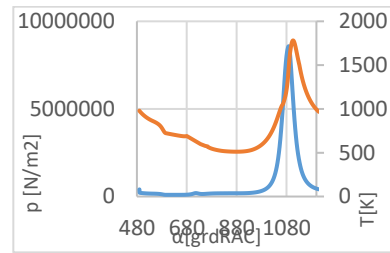


Fig. 4.6. The pressure and temperature inside the cylinder for the case of dual fuelling at the degree of substitution $x_c=39.25\%$.

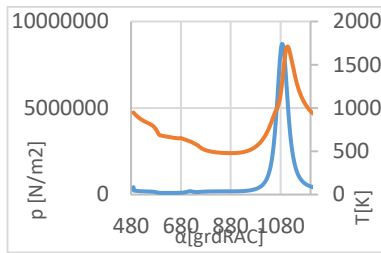


Fig. 4.4. The pressure and temperature inside the cylinder for the case of dual fuelling at the degree of substitution $x_c=8.14\%$.

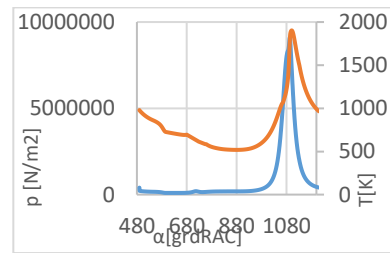


Fig. 4.7. Pressure and temperature inside the cylinder for the case of dual fuelling at the degree of substitution $x_c=51.57\%$.

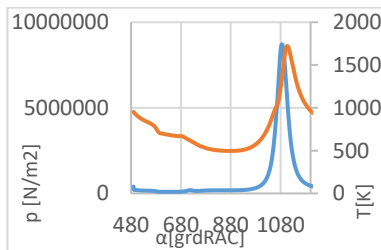


Fig. 4.5. Pressure and temperature inside the cylinder for the case of dual fuelling at the degree of substitution $x_c=25.11\%$.

For the maximum substitution degree, $x_c=51.57\%$, the in-cylinder pressure reaches a maximum of 91 bar at 4 CAD after the TDC, and the temperature reaches a maximum of 1902 K, at 21 CAD after the TDC, *figure 4.7*. *Figures 4.8 to 4.10* show the variation versus the coefficient x_c of LPG diesel substitution of the maximum pressure, the maximum pressure rise rate, the maximum temperature. The maximum pressure rise rate is slightly lower at the LPG fuelling (except $x_c=25.11\%$), *figure 4.9*.

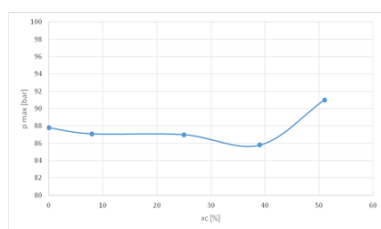


Fig. 4.8. Variation of the maximum pressure depending on the degree of substitution of diesel fuel with LPG

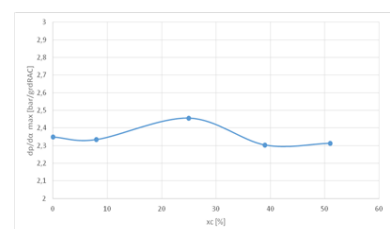


Fig. 4.9. Variation of the maximum pressure rise rate depending on the degree of substitution of diesel fuel with LPG

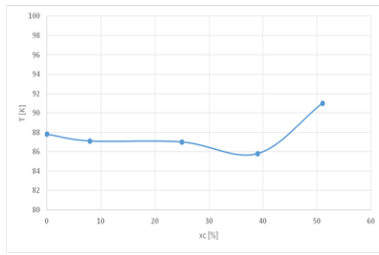


Fig. 4.10. Variation in the maximum temperature depending on the degree of substitution of diesel fuel with LPG.

Heat release rate

The heat release rate determined with the MUSA model is shown in *figure 4.11*. In the case of diesel fuel and LPG fuelling, there is a tendency to increase the rate of heat release for all degrees of substitution used compared to the diesel fuel use, $x_c=0\%$.

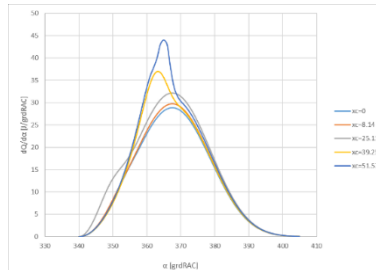


Fig. 4.11. The rate of heat release for the classic fuelling, $x_c=0\%$, and for the dual fuelling at different degrees of substitution.

For degrees of substitution $x_c=8.14\% \dots 25.11\%$, the rate of heat release reaches a maximum value higher by 6%... 17.5% compared to the classic fuelling, and for $x_c=39.25\%$ the maximum heat release rate increases by 33.9% compared to $x_c=0\%$. At the maximum degree of substitution, $x_c=51.57\%$, the maximum heat release rate increases by 56.7% compared to $x_c=0\%$. There is a trend of approaching 3...4 CAD closer to the TDC of the crankshaft rotation angle at which the maximum rate of heat release from the TDC occurs at $x_c=39.25\% \dots 51.57\%$ as the cyclic dose of LPG is increased, a trend correlated with increased maximum pressure and maximum temperature. The tendency to increase the maximum rate of heat release by the coefficient x_c of substitution of diesel fuel with LPG and its achievement earlier in the cycle, is due to the increase in the share of rapid combustion and the increase in the lower calorific value of the air-fuel mixture as diesel fuel is substituted by LPG.

4.1. MODELING OF FUEL VAPORIZATION, MIXING AND COMBUSTION PROCESSES WITH A DEVELOPED ONE-ZONE ZERO-DIMENSIONAL PHYSIC-MATHEMATICAL MODEL – SVAP MODEL

The one-zone thermodynamic model used to study the vaporization and combustion of the diesel droplet, a model called by the author SVAP, allows to estimate the influence of the degree of substitution of diesel fuel with LPG on processes such as vaporization, mixing and combustion, in order to deepen the analysis of the combustion process in the cylinder of the diesel engine fuelled with diesel fuel and LPG in dual mode. The SVAP model was developed for the same defined operating regime of 40% load and speed of 3900 rpm.

The model uses pressure charts acquired experimentally at the specified operating mode, *figure 4.13*, using averaged pressure diagrams from 250 individual pressure diagrams recorded for consecutive cycles.

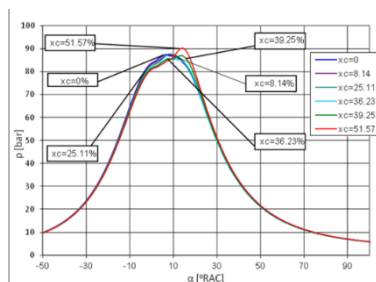


Fig. 4.13. Experimentally acquired pressure diagrams, averaged, at the 40% load and speed regime of 3900 rpm

In order to assess the current level of temperatures in the combustion chamber, the value of the global conventional temperature of the in-cylinder gases was determined at each degree of substitution, with the resolution related to the acquisition of pressure data, of 1 CAD.

The global conventional temperature in the cylinder, estimated on the basis of the state equation for each degree of substitution used, is shown in *figure 4.14*.

In this case, too, the tendency to increase the maximum temperature values when increasing the degree of substitution, x_c , *figure 4.15*, a trend also noted in the results determined by modeling for the temperature in the cylinder, is also noted.

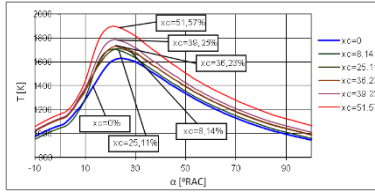


Fig. 4.14. Global combustion temperature at 40% load and speed of 3900 rpm

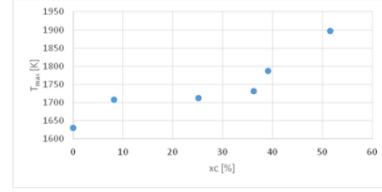


Fig. 4.15 Variation of the maximum temperature with the degree of substitution at the regime of 40% load and speed of 3900 rpm

Compared to diesel fuel use, the heat release rate (VDC), *figure 4.16*, increases by up to 46% on dual fuel mode for maximum substitution.

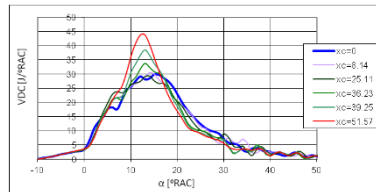


Fig. 4.16 Heat release rate at operating regime of 40% load, 3900 rpm speed.

For the study of the processes of vaporization, mixing with air and combustion at the level of the liquid fuel jet, the case of a droplet with a diameter of 10 μm is considered, a specific value for the diesel fuelling system of the K9K 1.5 dCi diesel engine where the injection pressure reaches **1600** bar and the diameter of the nozzle hole is **0,15** mm.

Calculation of the time of fragmentation of the diesel fuel jet

The variation in the fragmentation time of the diesel jet into droplets with a diameter of 10 μm at varying degrees of LPG diesel substitution is shown in *figure 4.17*. When fuelling in dual mode is used, the fragmentation of the diesel jet into droplets is done faster as a result of the reduction of the cyclic amount of diesel fuel, the fragmentation time of the diesel jet (TFJ) into droplets being reduced by about **18.2%** to $x_c = 51.57\%$ compared to the diesel fuel use.

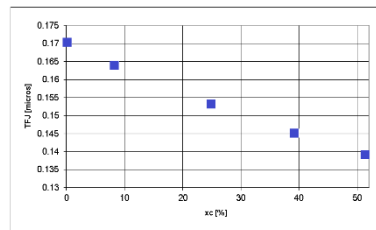


Fig. 4.17 The fragmentation time of the diesel fuel jet into droplets with a diameter of 10 μm .

The other degrees of substitution also record values lower by 4.11% at $x_c=8\%$, by 10.5% at $x_c=25\%$ and by 14.7% at $x_c=39\%$ for the diesel jet fragmentation time.

Calculation of the vaporization time of diesel fuel droplets in the air-LPG mixture

The vaporization time of the diesel droplet is reduced by 3.3% to $x_c=51.57\%$, *figure 4.18*, but also at the other degrees of substitution the time required to vaporize the diesel droplet is lower compared to the values set for the classical fuelling, the combustion of the air-LPG mixtures favoring the vaporization of the diesel fuel droplets in the immediate vicinity, *figure 4.19*.

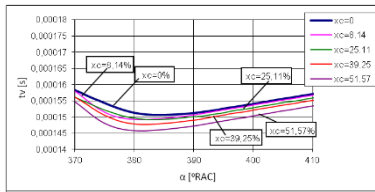


Fig. 4.18. The time of vaporization of the diesel fuel droplet in the presence of combustion of the air-LPG mixture, at different degrees of substitution.

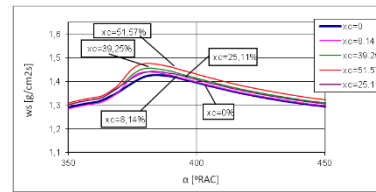


Fig. 4.19. The rate of vaporization of the diesel fuel droplet in the presence of combustion of the air-LPG mixture, at different degrees of substitution.

The flow of diesel fuel vapor formed at the surface of the considered droplet increases in the dual mode fuelling by up to 4.2%, to the degree of substitution $x_c=51\%$, compared to the standard feed. The combustion of air-LPG mixtures in the vicinity of diesel droplets accelerates the vaporization of the diesel fuel droplet resulting in a reduction in the droplet vaporization time and an increase in the flow of fuel vapor to the droplet surface.

Calculation of the mixture formation speed

The rate of air-diesel fuel mixing is increased in the case of dual mode fuelling compared to the standard fuelling, *figure 4.20*, due to the reduction in the amount of diesel fuel per cycle with the increase in the cyclic dose of LPG, but also due to the reduction of the fragmentation time of the diesel fuel jet into droplets, *figure 4.17* and the reduction of the time required for the vaporization of a droplet of diesel fuel, *figure 4.18*. For example, for the maximum degree of substitution, the speed of formation of the mixture between the air and the vaporized drop increases by 20.8% compared to the diesel fuel use, *figure 4.20*.

The final mass of the mixture of the cylinder, consisting of air-LPG-diesel fuel vapors, is formed in a shorter time, *figure 4.21*, and in a given time, it is 15 % higher than the value allocated to operation when diesel fuel is used, *figure 4.21*.

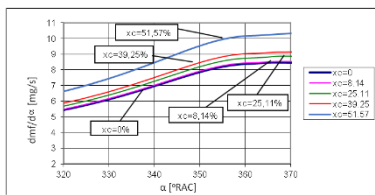


Fig. 4.20 The speed of formation of the mixture between air and the droplet of vaporized diesel fuel, at different degrees of substitution

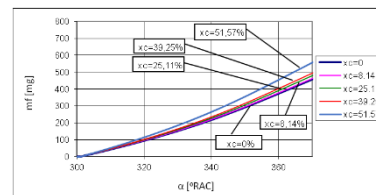


Fig. 4.21 The mass of the air-vapor mixture of diesel fuel-LPG formed at different degrees of substitution

Calculation of the drops combustion time

Figure 4.22 shows the variation in the combustion time of diesel fuel droplets in the air-LPG mixture in the cylinder for varying degrees of substitution. The presence of homogeneous air-LPG mixtures favors the combustion of diesel fuel droplets, at the maximum degree of substitution the combustion time of a diesel fuel droplet being 3.9% lower compared to the standard fuelling.

The reduction of the time allotted for the combustion of diesel fuel droplets is in line with the increase in the combustion rate of the diesel fuel droplet, at dual fuelling, *figure 4.23*.

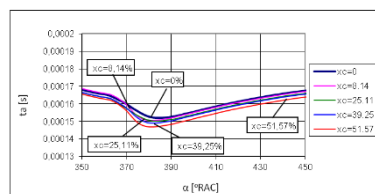


Fig. 4.22. The combustion time of diesel fuel droplets in the air-LPG mixture at different degrees of substitution

Calculation of the combustion speed

The increase in the mass flow rate of diesel fuel at the droplet surface, *figure 4.21*, leads to an increase in the rate of combustion of the diesel fuel droplet by up to 2,7 % at the dual fuelling for the maximum degree of substitution, *figure 4.23*.

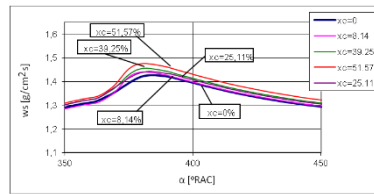


Fig. 4.23 The combustion speed of the diesel fuel droplet in the air-LPG mixture at different degrees of substitution

Calculation of the flame radius of diesel fuel droplet combustion in the air-LPG mixture

Figure 4.24 shows the values determined for the flame radius for the diesel fuel fuelling and the dual fuelling mode when diesel fuel and LPG are used, respectively.

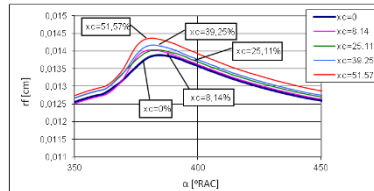


Fig. 4.24 Flame radius at combustion of the diesel fuel drops in the air-LPG mixture at different degrees of substitution

The increase in the flame radius and the combustion speed of diesel fuel droplets at dual fuelling correlates with the tendency to increase the heat release rate, pressure and global combustion temperature previously observed. The SVAP model is calibrated with experimental data, obtaining the law of combustion, figure 4.25, respectively the indicated diagram allocated to the operation at the use of diesel fuel, figure 4.26, established in the case of considering the combustion of the five jets of diesel fuel in the combustion chamber, at classic fuelling and at dual fuelling with diesel fuel and LPG.

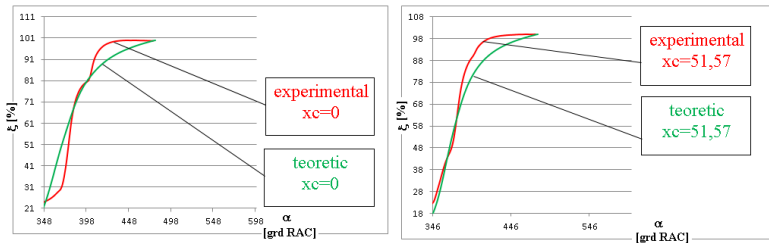


Fig. 4.25. Comparison of the combustion laws determined theoretically and experimentally, at the classical fuelling ($x_c=0\%$) and in the dual fuelling mode for the maximum cyclic dose of LPG ($x_c=51,57\%$), at the operating regime of 40% load and speed of 3900 rpm.

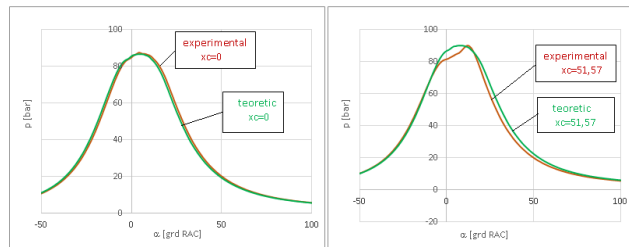


Fig.4.26. Comparison of pressure diagrams determined theoretically and experimentally at the operation in the case of diesel fuelling ($x_c=0\%$) and in dual fuelling mode for the maximum cyclic dose of LPG ($x_c=51,57\%$), at the operating regime of 40% load and speed of 3900 rpm.

Based on the previous relationship, the mass speed of smoke formation was determined, figure 4.27. In the case of diesel fuel fuelling, $x_c = 0\%$, the mass formation speed is the highest value. For the interpretation of the results, by integrating the formation velocities, the mass laws of soot formation were determined, figure 4.28.

The overall mass rate of combustion per unit area defined as the soot oxidation rate (VOF) determined for the speed of 3900 rpm and load regime of 40 % is shown for each degree of substitution in figure 4.29.

At dual fuelling with diesel fuel and LPG, for the maximum degree of substitution, the overall mass speed of soot oxidation reaches the highest maximum value, being 112.6% higher compared to $x_c=0\%$. Even from the use of lower cyclic doses of LPG, $x_c=8.14\%$, the oxidation rate of soot reaches a maximum of 52.4% higher than the standard supply, figure 4.29.

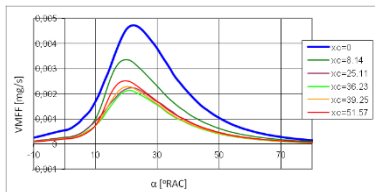


Fig. 4.27. Mass speed of smoke formation at speed 3900 rpm, load 40%.

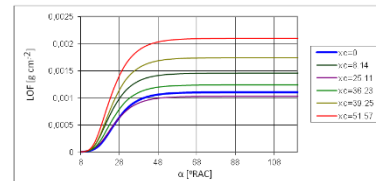


Fig. 4.30. The global law masses combustion per unit area at the speed regime 3900 rpm and load 40%.

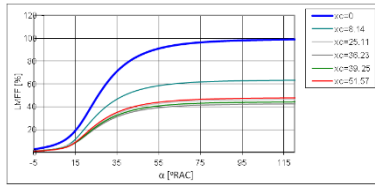


Fig. 4.28 Mass law of soot formation at speed 3900 rpm, load 40%, relative to condition $x_c=0\%$.

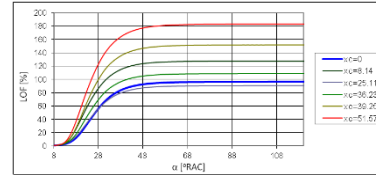


Fig. 4.31. The global mass law of combustion per unit area at speed regime 3900 rpm and load 40%, relative to condition $x_c=0\%$.

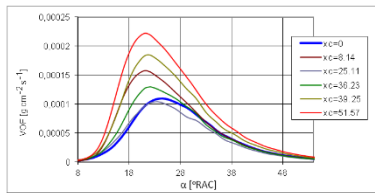


Fig. 4.29 Overall mass speed of combustion per unit area at speed regime 3900 rpm and load 40%.

In the standard fuelling mode, $x_c=0\%$, the oxidation of soot is established as the reference value. When feeding in a dual way, the amount of oxidized soot per unit area increases compared to the classical feeding situation, for most degrees of substitution, *figure 4.30* and *figure 4.31*.

In the conditions of the LPG fuelling in a dual mode, when the quantities of soot formed are reduced, and their oxidation is made more efficient compared to diesel, it results that the soot found in the exhaust gases is reduced by 28.7% to $x_c = 8.14\%$, by 55% at $x_c = 25.11\%$, by 71.7% at $x_c = 36.26\%$, by 56% at $x_c = 39.11\%$ and by 58% at $x_c = 51.57\%$ compared to the classical fuelling, $x_c=0\%$, *figure 4.32*.

Figures 4.32 and 4.33 show the relative emission of smoke from the exhaust gases for the regime of 3900 rpm speed and 40% load. The values theoretically determined on the basis of the model are presented in comparison with the experimental results of the smoke number K, the values being related to the condition $x_c=0\%$.

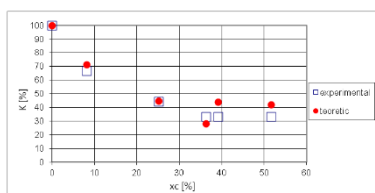


Fig. 4.32. The relative emission of smoke at the regime of 40% load and speed of 3900 rpm.

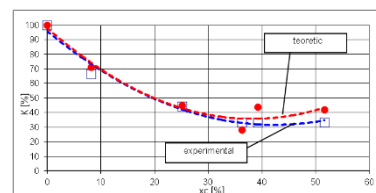


Fig. 4.33. The trend of variation of the relative emission of smoke at the regime of 40% load and speed of 3900 rpm.

A relatively small dispersion is recorded between the theoretically determined and the experimentally determined values. The theoretical study completes the experimental values in order to validate the tendency of variation of smoke emission from exhaust gases, when increasing the degree of substitution of diesel fuel with LPG.

Calculation of the nitrogen oxides emission level

At dual fuelling with diesel fuel and LPG, the use of relatively low degrees of substitution, $x_c=8\%$, $x_c=14\%$, $x_c=25.11\%$, $x_c=36.23\%$, leads to reaching maximum values of no formation speed lower by 23%, 29.2% and 22.1% respectively compared to the classical supply situation, *figure 4.34*.

Figure 4.35 shows the trend of variation in the relative level of emission of nitrogen oxides, NO, in relation to the condition $x_c=0\%$, depending on the value of the degree of substitution used in the 40% load and speed regime of 3900 rpm, experimentally.

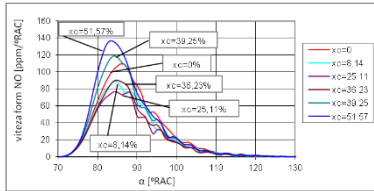


Fig. 4.34. NO formation speed, at varying degrees of substitution, at operating mode of 40 % load and speed 3900 rpm.

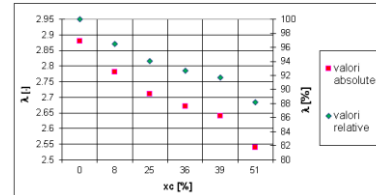


Fig. 4.36 The tendency of variation of the coefficient of excess air when increasing the degree of substitution of diesel fuel with LPG, at the operating regime 40% load and speed 3900 rpm

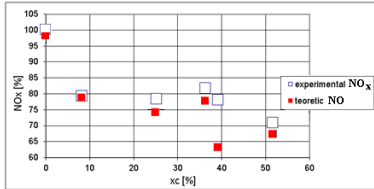


Fig. 4.35. Comparison of the theoretically and experimentally determined values of nitric oxide at varying degrees of substitution for the operating mode of 40 % load and speed 3900 rpm.

When the substitution rate of diesel fuel with LPG increases, the amount of liquefied petroleum gas injected into the intake manifold increases, which leads to a reduction in the excess air coefficient, *figure 4.36*, compared to the reference value found at $x_c=0\%$, by up to 11.8% for higher degrees of substitution ($x_c =40\% \dots 50\%$), because the amount of air admitted into the cylinder of the engine is reduced, so the formation of nitrogen oxides is hampered by the relative reduction of the oxygen available in the cylinder.

CHAPTER V

5. COMPARATIVE ANALYSIS OF THE RESULTS OF EXPERIMENTAL AND THEORETICAL INVESTIGATIONS

5.1. COMPARISON BETWEEN THEORETICAL RESULTS (MODELING OF THERMO-GAS-DYNAMIC PROCESSES IN THE CYLINDER OF THE K9K DIESEL ENGINE) AND EXPERIMENTAL RESULTS

5.1.1. In-cylinder pressure

In *figure 5.1*, the indicated pressure diagrams determined theoretically and experimentally for engine operation at fuelling with diesel fuel ($x_c=0\%$), respectively with diesel fuel and LPG at different degrees of substitution, x_c , are presented. The physic-mathematical model used has been calibrated so that there is a concordance between theoretical and experimentally determined results.

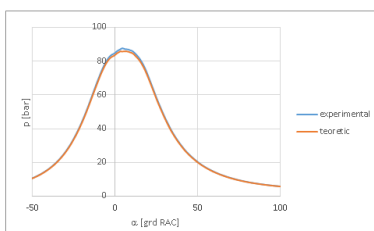


Fig. 5.1.a. Comparison of pressure charts determined theoretically and experimentally on the operation of the diesel fuelled engine ($x_c =0\%$)

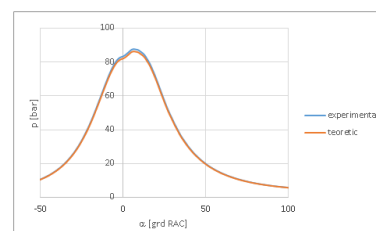


Fig. 5.1.c. Comparison of pressure charts determined theoretically and experimentally on the operation of the diesel fuel and LPG fuelled engine, at $x_c=25,11\%$

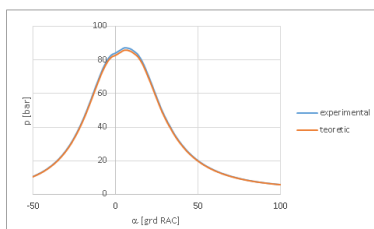


Fig. 5.1.b. Comparison of pressure charts determined theoretically and experimentally at the operation of the diesel fuel and LPG fuelled engine, at $x_c=8,14\%$

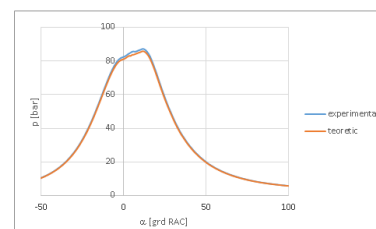


Fig. 5.1.d. Comparison of pressure charts determined theoretically and experimentally on the operation of the diesel fuel and LPG fuelled engine, at $x_c=39,25\%$

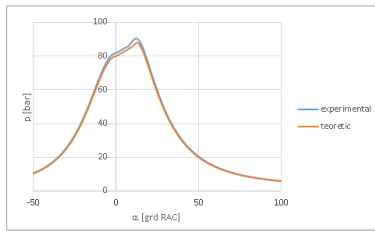


Fig. 5.1.e. Comparison of pressure diagrams determined theoretically and experimentally to the engine operation at the use of diesel fuel and LPG, at $x_c=51,57\%$

It is noted the proximity between the experimental and theoretical values for the maximum pressure, the maximum pressure rise rate and the angle of maximum pressure.

5.1.2. The Combustion Law

The afferent values 5%, 10%, 50% and 90% MFB are expressed in CAD and are compared with the experimentally determined values, *figures 5.2., 5.3., 5.4, 5.5*, observing a good correlation between the calculated values and those determined experimentally both in terms of the range of the values obtained, but also of their tendency to change with the degree of substitution x_c , [9].

For the 5 % and 10 % MFB, the dispersion between theoretically determined and experimentally determined values is relatively higher at some degrees of substitution. However, the study completes the experimental values from the point of view of validating the tendency of variation of the moment of beginning of the heat release (of the combustion process) to the increase of the degree of substitution of the classical fuel with liquefied petroleum gas, *figure 5.2 and figure 5.3*.

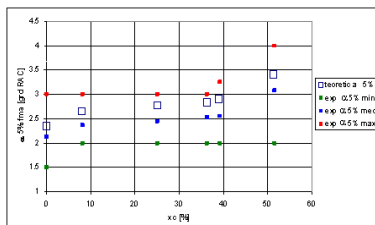


Fig.5.2. Comparison of 5% MFB calculated with thermodynamic model based on averaged pressure diagrams and experimentally determined for different degrees of LPG which substitute the diesel fuel

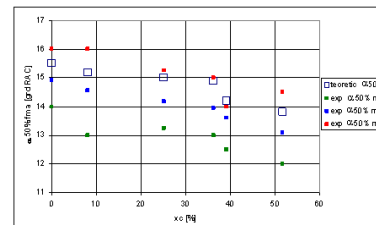


Fig. 5.4. Comparison of 5% MFB calculated with thermodynamic model based on averaged pressure diagrams and experimentally determined for different degrees of LPG which substitute the diesel fuel

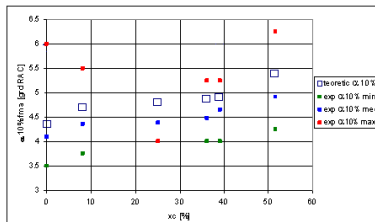


Fig. 5.3. Comparison of 5% MFB calculated with thermodynamic model based on averaged pressure diagrams and experimentally determined for different degrees of LPG which substitute the diesel fuel

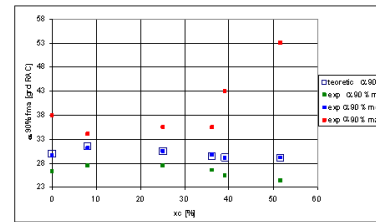


Fig. 5.5. Comparison of 5% FMA calculated with thermodynamic model based on averaged pressure diagrams and experimentally determined for different degrees of LPG which substitute the diesel fuel

For 50% and 90% of the MFB, the best correlations are obtained between the calculated values with the one-zone model used and the experimentally determined values, the dispersion between the calculated and experimental values being extremely low, *figure 5.4. and figure 5.5*. The fraction of 50% of the heat released per calculated cycle is found closer to the maximum values in the individual cycles, *figure 5.4.*, but the trend of variation with the degree of substitution x_c is similar. The final moment of combustion, specified by the calculated values for 90% MFB, *figure 5.5.*, is found almost identically among the average values measured in the individual cycles, at which the tendency of variation is identical.

5.1.3. NO emission concentration

Using the one-zone combustion model, the trend of variation of nitrogen monoxide, NO, in the exhaust gases can be estimated and the variation trend established in this way can be compared with the experimentally determined trend of variation for NO_x the calculated concentration of nitrogen monoxide emission is lower than that measured, since the gas analyzer measured the emission of nitrogen oxides as a whole (nitrogen monoxide, nitrogen dioxide, etc.).

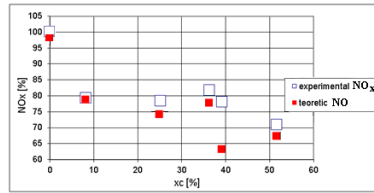


Fig. 5.6. Comparison of the theoretically and experimentally determined values of nitrogen oxides at different degrees of LPG which substitute the diesel fuel

Figure 5.6 shows the trend of variation in the relative level of emissions of nitrogen oxides, NO, and NO_x in relation to condition $x_c=0\%$, depending on the value of the degree of substitution used in the 40 % load and speed regime of 3900 rpm, determined theoretically (NO) and experimentally (NO_x).

Theoretically determined values show the same tendency of variation in increasing the degree of substitution. The dispersion between theoretically determined and experimentally determined values is relatively low, 6,8%.

5.1.4. Concentration of smoke emissions

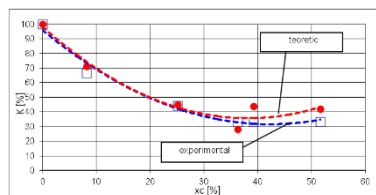
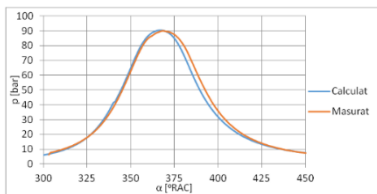


Fig.5.7. Comparison of theoretically and experimentally determined smoke emission values at different degrees of LPG which substitute the diesel fuel

Between the theoretically determined and experimentally determined values, a relatively small dispersion is recorded, being validated the tendency of variation of the smoke emission from the exhaust gases when increasing the degree of substitution of diesel fuel with LPG established by modelling.

5.2. COMPARISON BETWEEN THE RESULTS OBTAINED BY MODELING THE THERMO-GAS-DYNAMIC PROCESSES IN THE CYLINDER OF THE K9K ENGINE WITH THE AVL BOOST MODEL AND THE EXPERIMENTAL RESULTS

The individually determined pressure diagrams corresponding to the AVL Boost model are presented compared to the experimental pressure charts, in p - α coordinates. Figure 5.14 shows the variation of the pressure in the cylinder in the case of the classical fuelling, with diesel fuel, at the regime of 40% load and speed of 3900 rpm. A good proximity between the experimental and theoretical data can be observed, the recorded differences being less than 1%. For substitution degrees $x_c=8.14\%$, 25.11%, 39.25% and 51.57% the differences between the experimentally determined pressure variation and theoretically do not exceed 0.5%, *the figures from 5.15 to 5.18.*



Be g.5.14. The in-cylinder pressure diagrams for diesel fuel use, determined experimentally and by calculation with the AVL model, at the regime of 40% load and speed of 3900 rpm.

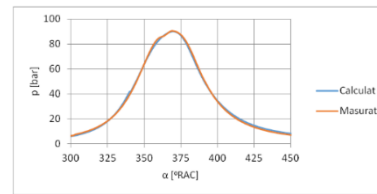


Fig. 5.16. The in-cylinder pressure diagrams at dual fuelling use for the degree of substitution 25,11%, determined experimentally and by calculation with the AVL model, at the regime of 40% load and speed of 3900 rpm.

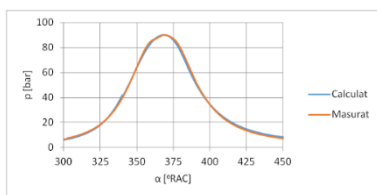


Fig. 5.15. The in-cylinder pressure diagrams at dual fuelling use for the degree of substitution 8,14%, determined experimentally and by calculation with the AVL model, at the regime of 40% load and speed of 3900 rpm.

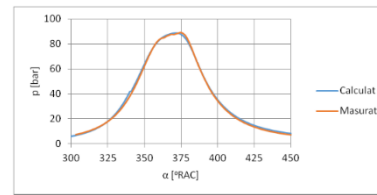


Fig. 5.17 The in-cylinder pressure diagrams at dual fuelling use for the degree of substitution $x_c=39,25\%$, determined experimentally and by calculation with the AVL model, at the regime of 40% load and speed of 3900 rpm.

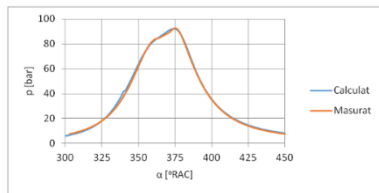


Fig. 5.18 The in-cylinder pressure diagrams at dual fuelling use for the degree of substitution $x_c=51,57\%$, determined

experimentally and by calculation with the AVL model, at the regime of 40% load and speed of 3900 rpm.

5.3. CONCLUSIONS

From the comparative analysis of the theoretical results obtained by modeling and the results of the experimental investigations, the following conclusions can be formulated: *the burnt mass fraction, established at the conventional values of 5%, 10%, 50% and 90% of the heat released on the cycle, theoretically determined with the one-zonal model, is found in the field established between the minimum and maximum values determined experimentally, the theoretical values following the tendency of variation of the experimental average values, noting a relatively small dispersion between them; Using the rate of heat release, the pressure variation in the cylinder can be established later, the values established with the designed one-zonal models being significantly close to the experimental values, similar correlations being obtained with the quasi-dimensional model AVL, with errors below 1%; The experimentally recorded trend of decrease in smoke and nitrogen oxide emissions, in a limited range of variation in the degree of substitution, can be explained by means of one-zonal models designed, by the combined effect of the pressure and temperature of the flue gases, a trend which is also found in the values established with the quasi-dimensional model AVL; Between the results of theoretical investigations and the results of experimental investigations there is an extremely small dispersion, thus being validated the thermodynamic models used.*

CHAPTER VI

6. CONCLUSIONS, PERSONAL CONTRIBUTIONS, FUTURE DIRECTIONS OF RESEARCH. DISSEMINATION OF THE RESULTS OF THE RESEARCH CARRIED OUT

6.1. CONCLUSIONS

General conclusions: *The level of NO_x emission decreases by 42% due to the reduction of the amount of oxygen available and the reduction of the gas temperature when increasing the degree of substitution of diesel fuel with LPG, at the regime of 85% load and speed 2000 rpm; at partial load 40% and speed 3900 rpm, the level of NO_x emission is reduced by a maximum of 29% to $x_c = 21.57\%$. At the other degrees of substitution, the NO_x emission level is reduced by up to 21,5 % compared to the NO_x emission level measured when the engine is operated on the diesel fuelling. At 55% load and 3900 rpm, at dual fuelling the NO_x emission level is continuously reduced by up to 17.7% to x_c maximum compared to $x_c=0\%$. At 70% load and 3900 rpm, the NO_x emission level is continuously reduced by up to 22.3% when the degree of substitution is increased. The reduction in the level of nitrogen oxides can be explained by the reduction of the oxygen available in the cylinder with the increase in the dose of LPG injected into the engine intake and by the reduction of the duration of combustion and of reaching the maximum temperature of the gases, a duration much shorter than that required for the formation of nitrogen oxides due to the increase in the combustion rate of homogeneous air-LPG mixtures; The HC emission level decreases by 63% due to the high combustion speed of homogeneous air-LPG mixtures, at the regime of 85% load and speed 2000 rpm; at the 3900 rpm speed regime, the high-speed combustion of homogeneous air-LPG mixtures ensures the reduction of HC emission by up to 52.5% at 40% load, by up to 85.7% at 55% load and by 98.3% at 70% load, respectively. Reducing the level of HC emissions also contributes to reducing the amount of carbon in the final mixture with increasing the degree of substitution of diesel fuel with liquefied petroleum gas; The level of smoke emission, assessed by smoke number K, is reduced by 30% due to the reduction of the carbon content and the high combustion speed of homogeneous air-LPG mixtures, at the regime of 85% load and speed 2000 rpm; At the 40% load regime, the opacity is reduced by up to 67.5%, to $x_c=21.57\%$ compared to the classical fuelling, the reduction being important, of 62.5% and to the maximum degree of substitution, $x_c=39.14\%$. The smoke number K is reduced by up to 66.6% on dual fuelling and maximum degree of substitution compared to the diesel fuel use, with more significant reductions being recorded as early range of the $x_c=21.57\% \dots 39.41\%$ of the degree of substitution. At the dual fuelling, at the 55% load*

regime, the level of exhaust gas opacity is reduced by 50% ($x_c=0.5\%$) compared to the classic fuelling. At this load regime, the smoke number K is reduced by 55.5% at the dual fuelling for the maximum degree of substitution. At the 70% load regime, compared to the classic fuelling, at the engine fuelled with diesel fuel and LPG appears a continuous reduction of the level of exhaust gas opacity by up to 39.13% at $x_c=0.5\%$, the reductions being more significant after $x_c=0.3\%$, in the range $x_c=0.31\%...0,51\%$. The smoke number, the K value, is reduced by up to 45.4% at the dual fuelling.

The sharp decrease in the level of polluting emissions, of the emission of carbon dioxide and the reduction of the specific energy consumption to the increase of the degree of substitution of diesel fuel with LPG, confirms the achievement of the objectives of the elaborated work and thus underlines the premises of the use of the diesel car engine in the conditions of the new *green deal* policy.

6.2. PERSONAL CONTRIBUTIONS

The author's personal contributions to the preparation of the doctoral thesis are: *Updating the present state of research in the field of LPG use in diesel engines by synthesizing information in the field; Modernization of the stand of experimental investigations of the engine. Upgrade of the electric dyno control unit; Establishing the procedure for conducting experimental investigations of the diesel engine fuelled with LPG in dual mode; Adaptation of a one-zone physic-mathematical model for simulation of the in-cylinder processes of the engine fuelled with diesel fuel and LPG in dual mode; Modeling of the processes of spraying, vaporization of diesel droplets and formation of air-diesel fuel mixture; Validation of the physic-mathematical model used by comparative analysis of the results of experimental and theoretical investigations performed.*

6.3. FUTURE DIRECTIONS OF RESEARCH

Future directions of research are the following: *Implementation of the LPG fuelling solution of the engine on car board and performing experimental investigations in real track conditions, at load regimes and engine speeds which are frequently used in operation; The use of LPG direct injection into the engine cylinder; Establishing optimal solutions for tuning the diesel fuel injection timing, diesel pilot quantity, LPG consumption, dosage, etc., at different operating regimes; Greening of the diesel engine at LPG use by using solutions to neutralize CO_2 and NO_x .*

SELECTIVE BIBLIOGRAPHY

- [1] *D.P. von Rosenstiel, D.F. Heuermann, S. Hüsig*, Why has the introduction of natural gas vehicles failed in Germany?—lessons on the role of market failure in markets for alternative fuel vehicles, *Energy Pol.*, 78 (2015), pp. 91-101, [10.1016/j.enpol.2014.12.022](https://doi.org/10.1016/j.enpol.2014.12.022)
- [2] *M.E.J. Stettler, W.J.B. Midgley, J.J. Swanson, D. Cebon, A.M. Boies*, Greenhouse gas and noxious emissions from dual fuel diesel and natural gas heavy goods vehicles, *Environ. Sci. Technol.*, 50 (2016), pp. 2018-2026, [10.1021/acs.est.5b04240](https://doi.org/10.1021/acs.est.5b04240)
- [4] *Liviu Nemoianu, Alexandru Cernat, Constantin Pană, Niculae Negurescu, Cristian Nuțu*, Study of the Diesel Cycle Variability at LPG Fuelling-MATEC Web of Conferences 2017;112:10006, DOI: 10.1051/mateconf/201711210006.e10006
- [8] *C. Pană, N. Negurescu, M. G. Popa, A. Cernat*, Experimental Aspects of the Use of LPG at Diesel Engine, *Scientific Bulletin of UPB, Seria D*, 1, 2010
- [9] *Marcel Ginu Popa, Niculae Negurescu, Constantin Pană*, Diesel Engines. Processes, vol I , II, Publisher Matrix Rom Bucharest, 2003
- [10] *Niculae Negurescu, Constantin Pană, Marcel Ginu Popa*, Internal Combustion Engines, vol II, Publisher Litografia I.P.B.. 1985
- [11] *Constantin Pană, Niculae Negurescu, Marcel Ginu Popa, Alexandru Cernat, Dorin Soare*, Dual alternative fuelling system for the greening of the automotive diesel engines, Research Contract no. 3812
- [12] *Pana, C., Negurescu, N., Popa, M. G., Cernat, Al., Despa, P., Bujgoi, Fl.*, „Aspects of the LPG Use in Diesel Engine by Diesel-Gas Method”, FISITA World 2008, Munchen, 2008.
- [13] *Cernat Alexandru*, Contributions to the study of the diesel engine running at fuelling with diesel fuel and LPG, PhD Thesis, UPB, 2010
- [16] *Pischinger F., Menne R.*, Dieselzweistoffbetrieb mit Flüssigeinspritzung von Propan/Butan ins Ansaugrohr, *MTZ* 40 (1979), nr.3
- [18] *Goto S, Lee D., Wakao Y., Honma H., Mori M., Akasaka Y., Hasimoto K., Motohashi M., Konno M.*, Development of an LPG DI Diesel Engine Using Cetane Number Enhancing Additives – SAE Paper 1999-01-3602, *Alternative Fuels* 1999, SP-1482

- [19] *Kajitani S., Chen C.L., Oguma M., Alam M., Rhee K.T.*, Direct injection Diesel Engine Operated with Propane – DME Blended Fuel, SAE Tehnical Paper Series 982536
- [20] *Negurescu N., Pana, C., Popa, M. G., Racovitză Al.*, Research on LPG Fuelling Diesel Engine, AMMA 2002, Cluj-Napoca
- [21] *Pana C., Negurescu N., Popa M. G., Cernat Al.*, Researches regarding the use of LPG at diesel engine, UPB-MASTER SA Research contract no. 24-01-03/2001
- [25] *Fujimoto, K., Congming, L., Xingdong, Y., Muroi, T., Yoshino, K.*, Production of Liquefied Petroleum Gas (LPG) from Biomass or Biogas, Japan Gas Synthesis Co. LTD., Japan 9th Biomass Asian Workshop 2012.12.3-4
- [26] ***<http://www.instalatiiigplpitesti.ro/instalatii-auto-de-gaz-gpl/injectie-mecanica>
- [27] *L. Nemoianu, C. Pana, N. Negurescu, A. Cernat, D. Fuiiorescu and C. Nutu*, On LPG use at diesel engine: pollutant emissions level and cycle variability aspects, IOP Conference Series: Materials Science and Engineering, <http://iopscience.iop.org/article/10.1088/1757-899X/444/7/072002> -.
- [28] *Pedessac J and Dagnas F X*, GPL Carburant: un carburant propre d'aujourd' hui et pour demain, Comite Francais du Butane et du Propane (France),2004
- [29] *Bielaczyc P, Szczotka A and Brodzinski H*, Analysis of the Exhaust Emissions from Vehicles Fuelled with Petrol or LPG and CNG Alternatively, Journal of Kones. Combustion Engines 1-2 B pp 363-369, 2001
- [116] *Negurescu N., Pană C., Popa M.G.*, Internal Combustion Engines. Processes, Volume I, II, Publisher MatrixRom, Bucharest, 1996
- [117] *Ramos J.L.*, Internal combustion engine modelling, Hemisphere Publishing Corporation, 1989.
- [118] *Hohenberg G.*, Berechnung des gaseitigen Wärmeubertganges in Dieselmotoren-MTZ 41(1980), nr 7/8.
- [119] *Apostolescu N, Chiriac R*, Combustion process in Internal Combustion Engine-Fuel Economy and Emission Reduction, Publiher Tehnică, Bucharest, 1998